Special Section:
Advances in scaling and modeling of land-atmosphere interactions

Key Points:

- Emissions differ greatly between crop species in pattern and strength and also vary with weather conditions and phenological development
- Potential impacts on air chemistry vary strongly with species and depend on compound reactivity in addition to source strength of emissions
- Data suggest that models should better consider growth developmental stages in order to better represent the seasonality of crop emissions

Supporting Information:

Supporting Information may be found in the online version of this article.

Correspondence to:

R. Grote,
ruediger.grote@kit.edu

Modeling Intra- and Interannual Variability of BVOC Emissions From Maize, Oil-Seed Rape, and Ryegrass

Felix Havermann[1,2], Andrea Ghirardo[3], Jörg-Peter Schnitzler[3], Claas Nendel[4,5,6], Mathias Hoffmann[4], David Kraus[1], and Rüdiger Grote[1]

[1]Karlsruhe Institute of Technology, Institute of Meteorology and Climate Research–Atmospheric Environmental Research, Garmisch-Partenkirchen, Germany, [2]Now at Department of Geography, Ludwig-Maximilians-Universität München, Munich, Germany, [3]Research Unit Environmental Simulation (EUS), Helmholtz Zentrum München, Institute of Biochemical Plant Pathology, Neuherberg, Germany, [4]Leibniz Centre for Agricultural Landscape Research (ZALF), Müncheberg, Germany, [5]Institute of Biochemistry and Biology, University of Potsdam, Potsdam, Germany, [6]Global Change Research Institute of the Czech Academy of Sciences, Brno, Czech Republic

Abstract   Air chemistry is affected by the emission of biogenic volatile organic compounds (BVOCs), which originate from almost all plants in varying qualities and quantities. They also vary widely among different crops, an aspect that has been largely neglected in emission inventories. In particular, bioenergy-related species can emit mixtures of highly reactive compounds that have received little attention so far. For such species, long-term field observations of BVOC exchange from relevant crops covering different phenological phases are scarcely available. Therefore, we measured and modeled the emission of three prominent European bioenergy crops (maize, ryegrass, and oil-seed rape) for full rotations in north-eastern Germany. Using a proton transfer reaction–mass spectrometer combined with automatically moving large canopy chambers, we were able to quantify the characteristic seasonal BVOC flux dynamics of each crop species. The measured BVOC fluxes were used to parameterize and evaluate the BVOC emission module (JJv) of the physiology-oriented LandscapeDNDC model, which was enhanced to cover de novo emissions as well as those from plant storage pools. Parameters are defined for each compound individually. The model is used for simulating total compound-specific reactivity over several years and also to evaluate the importance of these emissions for air chemistry. We can demonstrate substantial differences between the investigated crops with oil-seed rape having 37-fold higher total annual emissions than maize. However, due to a higher chemical reactivity of the emitted blend in maize, potential impacts on atmospheric OH-chemistry are only 6-fold higher.

Plain Language Summary   For evaluating the air quality, it is important to know what kind of chemical compounds are emitted from plants into the atmosphere. Such emissions vary widely by plant type and species, including agricultural crops. These differences have not been sufficiently accounted for because long-term field observations from relevant crops are scarcely available. Therefore, we measured and modeled the emission of three prominent European crops (maize, ryegrass, and oil-seed rape) for full rotations in north-eastern Germany. Using the measurements for parametrization, we simulated each measured compound individually and also evaluated the importance of these emissions for air chemistry. We can now demonstrate substantial differences between the investigated crops. For example, on an annual basis, oil-seed rape emitted 37-fold more overall emissions than maize, but since the emitted compounds are less reactive, its effect on air chemistry is only 6-fold higher.

1. Introduction

Vegetation plays a pivotal role in the exchange of trace gases between the land surface and the atmosphere. The emissions of biogenic volatile organic compounds (BVOCs) with a global mean of 760 TgC a^{-1} (1980–2010), exceed those from anthropogenic sources with around 110 TgC a^{-1} (AVOCs, e.g., from transport, solvent use, production and storage processes, and combustion processes) by far (Calfapietra et al., 2013; Piccot et al., 1992; Sindelarova et al., 2014). In addition, BVOCs are generally more reactive than AVOCs. Once emitted into the air, BVOCs immediately start to oxidize with the hydroxyl radical (OH), ozone (O$_3$), nitrate radical (NO$_3$), and in coastal areas with chlorine (Cl) atoms, leading to first generation BVOC products (Peñuelas & Staudt, 2010). The reaction of BVOCs with OH is the dominant kind of BVOC decomposition in the troposphere, which is why the total BVOC–OH reactivity is generally used to quantify the emission impact on atmospheric chemistry

(Dominutti et al., 2019; Hakola et al., 2017; Hu et al., 2018). The consumption of OH radicals prolongs methane (CH_4) lifetime and thus indirectly enhances radiative forcing (Kaplan et al., 2006). Even in urban areas, the contribution of BVOCs to air chemistry can thus be relatively large although AVOC emissions are quantitatively more relevant (Abeleira et al., 2017; Simon et al., 2019; Zhao et al., 2019). For example, a case study in the Baltimore/Washington region found that during summer biogenic VOCs accounted for about half of total OH reactivity (Halliday et al., 2015). Intermediate products and subsequent later generation products lead to the formation of O_3 (photochemically under high NO mixing ratios) and secondary organic aerosols (SOA; Atkinson, 2000; Holopainen et al., 2017; Wang et al., 2018). While O_3 is directly toxic for plants and humans and also has strong impacts on air chemistry, SOA perturb the radiative transfer and support the growth of particles by acting as cloud condensation nuclei (CNN; Carslaw et al., 2013; Scott et al., 2014). Regarding O_3 formation, BVOCs were estimated to contribute around 50% to ozone formation in a Chinese urban area despite contributing only about 5% to total VOCs (ppbv, throughout a whole year; Song et al., 2019). Similarly, SOA concentrations over China have been estimated to originate predominantly (about 70%) from biogenic sources (Wu et al., 2020), although for specific regions and time periods, the fraction depends strongly on temperature, specific compounds, as well as the abundance of chemical reaction partners such as anthropogenic emissions.

The magnitude and compound composition of BVOC emissions from a particular plant or vegetation type depends on its genetical properties (i.e., emission capacity), while the actual emission rate and its dynamics depend on environmental conditions such as temperature, absorbed photosynthetic active radiation (PAR), ambient CO_2 concentration, as well as various biotic and abiotic stressors and the plant phenological state (Brilli et al., 2019; Grote, 2019; Manco et al., 2021; Niinemets & Monson, 2013). In particular, it is known that BVOC emissions from different species are highly divers in their chemical composition (Courtois et al., 2009; Monson et al., 2013). This variety is important to consider (Heald & Kroll, 2020) but not fully reflected in regional emission inventories that often pool various species of mixed ecosystems into one emission type (e.g., tropical forests, Nichol & Wong, 2011) or use the same emission assumptions for various (monospecific) land covers that have a similar management type (e.g., continental agricultural areas, Karl et al., 2009). These assumptions are challenged by findings that indicate a large regional variability in emission types within apparently similar forests (Gu et al., 2017) as well as different properties of crops, in particular those introduced for bioenergy production (Szogs et al., 2017). An additional aspect is that agricultural regions are subject to relatively fast changes in species selection and crop rotations. For example, the agricultural area used for maize plants in Germany has steadily increased during the last 30 years from 1.6 Mha (14%) in 1990 to 2.7 Mha (23%) in 2020 (https://www.destatis.de, Statistisches Bundesamt, 2021, last access: 30.06.2021). A similar development can be seen for oil-seed rape which increased from 0.7 Mha (6%) in 1990 to almost 1.5 Mha in 2010 (but decreased thereafter to about 1 Mha in 2020; https://www.destatis.de, Statistisches Bundesamt, 2021, last access: 30.06.2021). Considering that very different BVOC emission rates have been depicted for maize and oil-seed rape compared for example, with wheat (Gonzaga Gomez et al., 2019), it seems unreasonable to use a lumped emission factor for crops, in particular when longer periods should be investigated.

The change in species composition is partly driven by an increasing demand for fodder and bioenergy, favoring species such as maize, oil-seed rape and grass, which is a development projected to continue (Bentsen & Felby, 2012; Gelfand et al., 2020). However, knowledge about the composition of BVOC emissions and on their environmental drivers is still scarce for many of these plants. Particularly full seasonal BVOC observations that cover the whole range of phenological phases are hardly available, although the linkage of emissions to physiological processes and anatomical developments is decisive for simulations that aim to dynamically respond to various combinations of environmental conditions. It should also be considered that available information is often derived at regions where these species have been grown in the past, which have not been necessarily the same conditions than they experience under a central European climate. Therefore, we are presenting several weeks of observations in each of three different crop types (*Zea mays, Brassica napus, Lolium multiflorum*) that are already planted in Central Europe and/or are supposed to increase in importance. Since a detailed analysis of BVOC fluxes from maize have been presented before (Wiβ et al., 2017), we now concentrate on the comparison of the different crops, evaluating their potential impact on air quality. We therefore elaborate and parameterize a physiology-oriented BVOC emission model based on measurement results. Simulating not only developments during the observation period but also throughout a full three-year period, we present a comprehensive comparison of intensity and quality of BVOC emissions for the three investigated species.

Table 1
Plant Species, Date of Seeding and Harvest, Measurement Period, Number of Chambers

Plant species	Common name (cultivar)	Seeding	Harvest	BVOC measurement period	CO_2 measurement period	N data (daily/ hourly)	N chambers
Zea mays L.	Maize (Zoey)	29.4.2015	14.9.2015	24.07.2015–16.09.2015	04.2015–09.2015	48/1153	2
Brassica napus L.	Oil-seed rape (Pr44d06)	20.8.2015	19.5.2016	09.04.2016–20.05.2016	08.2015–07.2016	29/801	4
Lolium multiflorum L.	Ryegrass (Country 2051)	25.8.2016	17.5.2017, 26.06.2017, 04.08.2017	09.06.2017–29.06.2017	08.2016–09.2017	16/396	4

2. Materials and Methods

2.1. Field Observations

Three intensive measurement campaigns were carried out throughout 2015–2017 at an agricultural field site close to the research station Dedelow, located in north-eastern Germany (N 53.3793, E13.7856). In each of the 3 years, a different crop (maize (*Zea maize*), oil-seed rape (*Brassica napus*), and ryegrass (*Lolium multiflorum*)) has been investigated (see Table 1 for management and observation details). The meteorological conditions during the three years were similar with respect to temperature and radiation conditions (average 9.6, 9.8, and 9.5°C for 2015, 2016, and 2017 respectively). Only minor interannual variations could be detected such as a relatively cool early April but a warm August in 2015, warm periods in January/February and September in 2016, as well as a cool late April but warm October in 2017 (see meteorological developments in the supplements Figure S1-S3 in Supporting Information S1). However, precipitation was different in the three years (annual rainfall of 475, 392, and 755 mm for 2015, 2016, and 2017 respectively) with 2017 showing exceptional high rainfall rates particularly during June and July. In each year 160/0 (maize), 80/90 (oil-seed rape), or 0/160 (grass) kg N ha^{-1} was added to the site as urea and calcium-ammonium nitrate, respectively. Fertilization as well as application of herbicides, fungicides and insecticides (for maize and oil-seed rape) was carried out well before the start of the measurements. The agricultural site is embedded within the CarboZALF project (Sommer et al., 2016) which provides meteorological information, as well as the facilities for automatically controlled closed-chamber measurements.

In the following we briefly present the setup and execution of measurements as well as calculations, while a more detailed description can be found in Wiβ et al. (2017). All gas exchanges were derived from concentration measurements within large polycarbonate automatic chambers of 1.5 m × 1.5 m × 2.5 m size each. The chambers are mounted onto a steel frame and lifted or lowered by a cable winch (Hoffmann et al., 2017). An aliquote of the air was sampled (and re-added) while the chamber was closed (otherwise the chambers were kept open), thereby maintaining a flow-through nonsteady state system, and fluxes are calculated from the difference in concentration during the closure, which is less than 15 min in order to minimize the influence on environmental conditions. CO_2 and water concentrations were determined using an infrared LI-840 gas analyzer (LICOR Bioscience, Lincoln, Nebraska, USA) and a Campbell 500 data logger (see also Hoffmann et al., 2015). Air was drawn from the chamber at an airflow rate of 10 dm^3 min^{-1} and redirected into it except for a minor fraction (70 cm^3 min^{-1}) that was used for BVOC detection using a PTR-QMS 500 (Ionicon Analytik GmbH, Innsbruck, Austria). Overall, 18, 25, and 32 compounds were measured for maize, oil-seed rape, and ryegrass, respectively, covering *m/z* values between 21 and 225. All compounds with less than mean flux rates of 0.01 nmol m^{-2} s^{-1} were neglected in further analyses. For compound identification, additional air samples were collected and analyzed by gas chromatography mass spectrometry (GC-MS (GC type: 7890A; MS type: 5975C; both from Agilent Technologies, Palo Alto, CA, USA). Please note that isoprene and monoterpene fragments can be omitted from the analysis as their emission rates are based on measurements of the parent ions and quantified using certified standards.

BVOC fluxes were calculated as the slope of a linear regression (ordinary least squares), fitted to the concentration measurement points over time obtained during 12 min of sampling. All fluxes from nonsignificant linear regressions (H0: slope of regression line is zero; $p > 0.05$; that is, $r^2 < 0.60$ for a two-tailed t distribution test with 12 data points) were set to zero. From all measurements within an hour, the mean fluxes and the standard emission factors (SEFs, emissions that can be expected at 1000 μmol m^{-2} s^{-1} PAR and 30°C) are derived by curve fitting via the Levenberg–Marquardt algorithm with nonlinear least squares using the Python SciPy library (https://sourceforge.net/projects/scipy/files/scipy/0.14.0/, last access: 30.06.2021).

2.2. Parameter Derivation of BVOC Modeling

Light-dependent BVOC emissions are represented as a fraction of the electron transport rate as proposed by Niinemets et al. (1999); a theoretical approach that is based not on the transport rate as such but on the excess of electrons (JJv model) has been suggested by Morfopoulos et al. (2014) and elaborated by Grote et al. (2014). Emissions that are assumed to origin from storages and therefore are temperature-dependent only, are simulated with an exponential relation suggested by Guenther et al. (1993). Since the electron transport dependencies in the JJv model only replace the modifiers for light and temperature in the Guenther model, it can directly be used with *SEF* parameters that have been derived from measurements and fitted with the Guenther equations.

BVOC Emissions (E_{BVOC}, calculated in ng g^{-1} DW aboveground biomass h^{-1}) can potentially origin from two different sources, namely from a direct production (de novo *emissions*) that is considering radiation and temperature as simultaneous influences, as well as from storages that only depend on (tissue) temperature T (well described with a simple exponential relationship suggested by Guenther et al. (1993)). Therefore, we derived *SEF* and the slope parameter *β*, combining both approaches and linking them using the parameter *LDF* (light dependent fraction, Equation 1), which in turn is determined by iterating from 0 to 1 (in steps of 0.1) selecting the ratio that best fitted emissions (Table 2).

$$E_{\text{BVOC}} = SEF_{\text{BVOC}} \cdot \left[\text{LDF} \cdot \frac{\gamma_{\text{ph}}}{\gamma_{\text{ph}_{\text{norm}}}} \cdot \frac{\gamma_{\text{en}}}{\gamma_{\text{en}_{\text{norm}}}} + (1 - \text{LDF}) \cdot \exp\left(\beta \cdot (T - T_S)\right) \right] \tag{1}$$

$$\gamma_{\text{ph}} = \left[c_1 + c_2 \cdot \max\left(-\Delta J_{\text{sat}}, J - J_v\right) \right] \cdot J \cdot \min\left(1, \frac{C_i}{\Gamma^*}\right) \tag{2}$$

$$\gamma_{\text{en}} = \frac{\exp\left(c_0 - \frac{\text{AE}_E}{R_G \cdot T}\right)}{1 + \exp\left(\frac{\Delta S \cdot T - \text{DAE}_E}{R_G \cdot T}\right)} \tag{3}$$

with γ_{ph}, $\gamma_{\text{ph\_norm}}$ as well as γ_{en}, $\gamma_{\text{en\_norm}}$ being the photosynthetic (Equation 2) and enzymatic (Equation 3) emission potentials at current and standard environmental conditions as described in Grote et al. (2014). Parameters T_S (standard temperature 303.15 K), c_0 (32 J mol^{-1}), AE_E (83129 J mol^{-1}), DAE_E (284600 J mol^{-1}), and ΔS (887.5 J mol^{-1} K^{-1}) are taken from Niinemets et al. (1999). The values for c_1 (0.1765e^{-3}), c_2 (0.0028e^{-3}) and ΔJ_{SAT} (34 µmol m^{-2} s^{-1}) are taken from Grote et al. (2014) and R_G is the universal gas constant (8.314 J mol^{-1} K^{-1}). The electron transport rate J (µmol m^{-2} s^{-1}), the electron flux required to support Rubisco-limited carbon assimilation J_v (µmol m^{-2} s^{-1}), the intracellular CO_2 concentration C_i (µmol mol^{-1}) and the CO_2 compensation point Γ^*(µmol mol^{-1}) are supplied by the photosynthesis model (under either actual or standard conditions (T = T_S, radiation = 1000 µmol m^{-2} s^{-1} photosynthetically active quantum flux density).

2.3. Biogeochemical Modeling

We employed the physiology-oriented BVOC emission model JJv according to Grote et al. (2014) coupled to the ecosystem module PlaMo^x (Kraus et al., 2016; Petersen et al., 2021) that runs on an hourly temporal resolution within the LandscapeDNDC model framework (Haas et al., 2013). The model framework provides dynamic crop growth that is calculated from photosynthesis (Farquhar et al., 1980; Leuning, 1995) and ecosystem respiration (Thornley & Cannell, 2000) in dependence on environmental conditions (including nitrogen supply and water availability). Allocation of carbon is distributed into different compartments according to development stage using species-specific parameters. The height of the crop depends on the biomass in the stalk compartment. Water balance is calculated based on the original DNDC model (Holst et al., 2010; Li et al., 1992) and soil water contents below a certain threshold directly reduce photosynthesis.

All plant carbon exchanges (CO_2 as well as BVOCs) were calculated on an aboveground-biomass-basis according to the environmental conditions that are estimated within a specific canopy layer. Layers have a flexible thickness that depends on crop height, and leaf biomass is equally distributed between them. Foliage develops dynamically based on the calculation of growing degree day sums. Leaf area is directly related to leaf biomass by species-specific conversion factors (specific leaf area for maize, oil-seed rape and ryegrass are 16, 39.6, and 24.5, respectively). Since maximum carboxylation rate and electron transport rate are reduced proportionally to leaf

Table 2
BVOC Emission Parameter for Maize, Oil-Seed Rape, and Ryegrass Fitted to the Joint JJv–Pool Emission Model

m/z	Detected compound	Crop species	SEF	SE	LDF	β	R²	NSE
33	Methanol	Maize	n.s.[a]	n.s.[a]	n.s.[a]	n.s.[a]	n.s.[a]	n.s.[a]
		Oil-seed rape	5929	501	0.5	0.08	0.92	0.89
		Ryegrass	2104	233	0.8	0.06	0.36	0.34
45	Acetaldehyde	Maize	37.9	6.8	0.1	0.14	0.44	0.44
		Oil-seed rape	216	30	0.5	0.08	0.78	0.66
		Ryegrass	788	75	0	0.26	0.48	0.46
47	Ethanol	Maize	n.s.[a]	n.s.[a]	n.s.[a]	n.s.[a]	n.s.[a]	n.s.[a]
		Oil-seed rape	878	38	1	-	0.95	0.95
		Ryegrass	168	23	1	-	0.62	0.61
59	Acetone	Maize	56.9	9.3	0.2	0.13	0.59	0.58
		Oil-seed rape	444	21	0.8	0.08	0.96	0.95
		Ryegrass	365	29	0.9	0.09	0.69	0.68
61	Acetic acid	Maize	-		-	-	-	-
		Oil-seed rape	1638	106	0.9	0.12	0.84	0.78
		Ryegrass	n.s.[a]	n.s.[a]	n.s.[a]	n.s.[a]	n.s.[a]	n.s.[a]
69	Fragments[c]	Maize	25.5	4.3	0.2	0.13	0.43	0.43
	Isoprene	Oil-seed rape	454	28	1	-	0.89	0.81
		Ryegrass	98.7	9.3	1	-	0.49	0.46
71	u.m.f.[b]	Maize	18.0	4.1	0.2	0.17	0.33	0.33
	MACR/MVK	Oil-seed rape	214	12	0.9	0.1	0.93	0.9
		Ryegrass	9.1	2.2	1	-	0.2	0.09
73	u.m.f.[b]	Maize	-	-	-	-	-	-
		Oil-seed rape	397	20	0.9	0.11	0.94	0.91
	MEK	Ryegrass	94.2	11	1	-	0.81	0.72
79	u.m.f.[b]	Maize	-		-	-	-	-
		Oil-seed rape	138	12	1	-	0.74	0.69
		Ryegrass						
93	Toluene	Maize	-		-	-	-	-
		Oil-seed rape	166	10	1	-	0.86	0.83
		Ryegrass	-		-	-	-	-
99	Hexenal	Maize	39.7	7.4	0.2	0.15	0.56	0.56
		Oil-seed rape	248	18	1	-	0.87	0.83
		Ryegrass	88.2	11	1	-	0.77	0.55
101	Hexanal	Maize	102	20	0.2	0.15	0.59	0.57
		Oil-seed rape	824	49	0.8	0.12	0.88	0.84
		Ryegrass	70.8	12	1	-	0.36	0.34
107	Xylenes	Maize	11.8	3.0	0.2	0.13	0.45	0.45
		Oil-seed rape	158	9.2	1	-	0.92	0.89
		Ryegrass						
118	u.m.f.[b]	Maize	-		-	-	-	-
		Oil-seed rape	282	23	1	-	0.78	0.75
		Ryegrass	-		-	-	-	-

Table 2
Continued

m/z	Detected compound	Crop species	SEF	SE	LDF	β	R²	NSE
137	Limonene	Maize	157	36	0.3	0.13	0.4	0.39
	Thujene, Myrcene, trans-β-Ocimene	Oil-seed rape	562	33	1	-	0.87	0.83
	Myrcene	Ryegrass	49.9	7.0	1	-	0.6	0.46
151	DMNT	Maize	23.7	6.5	0.2	0.13	0.44	0.44
		Oil-seed rape	-		-	-	-	-
		Ryegrass	-		-	-	-	-
153	(E)-2-caren-4-ol, 4-ethylguaiacol, Camphor, MeSA	Maize	58.3	13	0.5	0.14	0.43	0.42
		Oil-seed rape	-		-	-	-	-
		Ryegrass	-		-	-	-	-
155	1,8-Cineole	Maize	15.7	2.6	0.3	0.15	0.65	0.64
		Oil-seed rape	-		-	-	-	-
		Ryegrass	-		-	-	-	-
205	α-Humulene	Maize	50.1	11	0.3	0.15	0.36	0.36
		Oil-seed rape	-		-	-	-	-
		Ryegrass	-		-	-	-	-

Note. Presented are standardized emission factors (SEF) with corresponding standard errors of the estimate (SE) both in ng g^{-1} DW aboveground biomass h^{-1}, the light dependent fraction (LDF) for partitioning between the JJv and pool emission algorithm, β-coefficient as a curvature parameter for the pool emission equation and the Nash-Sutcliffe modeling efficiency (NSE). All values are calculated for the whole measurement period. "-": no significant fluxes detected; MACR, Methacrolein; MVK, Methyl vinyl ketone; MeSA, Methyl salicylate; MEK, Methyl ethyl ketone; DMNT, Dimethyl nonatriene.
[a]n.s.: not simulated because of high deposition rates. [b]u.m.f.: unidentified mass feature. [c]fragments of Pentanal, Octanal, Nonanal, Decanal.

development and leaf senescence, also photosynthesis is decreased and precursor supply for BVOCs is reduced during this time. There are no other indirect seasonal effects on emission calculations.

Photosynthesis parameters, that is, those that influence the substrate provision for BVOC emissions, have been derived from literature for each of the investigated species (Table 3). BVOC simulation was carried out with the JJv model according to Equation 1 for all compound emissions that depend on light (Grote et al., 2014; Morfopoulos et al., 2014), using *SEF, β* and *LDF* values separately determined for all compounds as presented in Table 2. Thereby, compounds that are emitted from specific storages and thus showed no light dependence (LDF = 0) were solely calculated based on traditional storage-based emission schemes.

In order to derive the reactivity of the emission, we weighted the emission with the species-specific average blend for the whole season and multiplied with the depicted OH reactivity (Table 4). It should be noted that we excluded negative emissions, that is, potential deposition processes, from the analysis although these were sometimes substantial, in particular for oxygenated compounds when air humidity was high, and condensation on surfaces may have occurred. In these cases, deposition processes that are enhanced through solution into water can be expected.

We ran the coupled model with field-measured hourly weather data (temperature, radiation, precipitation) over the entire three years (2015–2017). The soil was initialized with measured values of soil structural properties down to 2 m depth (more than 50% sand and 10%–20% clay) from which pore space and water holding capacity were estimated. Simulations were carried out with the respective crop of the year starting with sowing date, considering a fertilization event before sowing. In addition, runs were set up for each year with every other crop so that crop development and BVOC emission could be compared under equal environmental conditions.

Finally, we estimated the importance of BVOC emissions for air chemistry by multiplying the emission of a specific compound *i* with its reaction rate coefficient with OH (Table 4). Using the simulations, we scaled the emissions up to a full growth period of each crop and compared them using the total BVOC–OH reactivity of maize as standard. Despite various non-linear dependencies in air chemistry, different rotation systems can still be compared with a simplified approach (Ghirardo et al., 2016; Graus et al., 2013; Hakola et al., 2017;

Table 3
Species-specific Photosynthesis Parameters Based on Literature

Parameter description	Abbreviation	Species	Values	Sources
Activation energy for electron transport (J mol⁻¹)	AEJM	Maize	77,900	Massad et al. (2007)
		Oil-seed rape	45,000	Groenendijk et al. (2011)
		Ryegrass	60,650	Yin et al. (2004)
Activation energy for Michaelis-Menten constant for CO_2 (J mol⁻¹)	AEKC	Maize	59,430	Yu et al. (2001)
		Oil-seed rape	59,356	Farquhar et al. (1980)
		Ryegrass	80,990	Bernacchi et al. (2002)
Activation energy for Michaelis-Menten constant for O_2 (J mol⁻¹)	AEKO	Maize	36,000	Yu et al. (2001)
		Oil-seed rape	35,948	Farquhar et al. (1980)
		Ryegrass	23,720	Bernacchi et al. (2002)
Activation energy for dark respiration (J mol⁻¹)	AERD	Maize	53,000	Yu et al. (2001)
		Oil-seed rape	66,405	Farquhar et al. (1980)
		Ryegrass	46,390	Bernacchi et al. (2001)
Activation energy for electron velocity (J mol⁻¹)	AEVC	Maize	67,294	Massad et al. (2007)
		Oil-seed rape	58,520	Farquhar et al. (1980)
		Ryegrass	65,330	Bernacchi et al. (2001)
Michaelis-Menten constant for CO_2 at 25°C (µmol mol⁻¹)	KC25	Maize	650	Von Caemmerer (2000)
		Oil-seed rape	460	Farquhar et al. (1980)
		Ryegrass	270	Bernacchi et al. (2002)
Michaelis-Menten constant for O_2 at 25°C (mmol mol⁻¹)	KO25	Maize	450	Von Caemmerer (2000)
		Oil-seed rape	330	Farquhar et al. (1980)
		Ryegrass	165	Bernacchi et al. (2002)
Maximum RubP saturated rate of carboxylation at 25°C (µmol m⁻² s⁻¹)	VCMAX25	Maize	125	Massad et al. (2007)
		Oil-seed rape	61	Dekker and Sharkey (1992)
		Ryegrass	68	Ainsworth and Rogers (2007)
Relation between maximum electron transport rate and RubP saturated rate of carboxylation (--)	QJVC	Maize	6.70	Massad et al. (2007)
		Oil-seed rape	3.07	Massad et al. (2007)
		Ryegrass	2.80	Ainsworth and Rogers (2007)
Photosynthesis curvature parameter (--)	Θ	Maize	0.70	Von Caemmerer (2000)
		Oil-seed rape	0.90	Thornley (2002)
		Ryegrass	0.90	Thornley (2002)

Hu et al., 2018; Sarkar et al., 2020), assuming that emissions are linearly proportional to BVOC concentration changes within the boundary layer (i.e., assuming a similar temperature response of BVOC reactivity with other air chemistry components). Another constrain is that the potential BVOC–OH reactivity could only be considered for those compounds which were identified by the GC-MS analysis, meaning that about 9.9% and 1.3% of emissions for maize and oil-seed rape, respectively, were neglected.

3. Results

3.1. Gross Primary Production and Biomass Development

The three species each showed specific growth patterns that were characterized by a relatively long growing period from May to October with growth starting to decline in about the middle of the period (maize), a dormancy during winter after a first growth and a relatively steep biomass increase between March and the end of June (oil-seed rape), and a continuous growth from March to August that is intermitted by cutting events in May, June, and early August (ryegrass; see Figure 1). Maize reached about 1.5 times the biomass of oil-seed rape (1.66 ± 0.1

Table 4
BVOC-OH Reaction Rate Coefficients (K-Rates) for Those Compounds Detected During the Field Campaigns Throughout 2015–2017

m/z	Detected compound	Compound group	OH *k*-rate
151	DMNT[c]	Homoterpenes	2.32×10^{-10}
137	Trans-β-Ocimene[a]	Monoterpenes	2.52×10^{-10}
	Myrcene[a]	Monoterpenes	2.15×10^{-10}
	Limonene	Monoterpenes	1.64×10^{-10}
69	Isoprene	Isoprene	1.00×10^{-10}
205	α-Humulene[a]	Sesquiterpenes	2.93×10^{-10}
	Isolongifolene[b]	Sesquiterpenes	9.60×10^{-11}
	Junipene[c]	Sesquiterpenes	6.21×10^{-11}
137	Thujene[c]	Monoterpenes	9.06×10^{-11}
99	Hexenal[a]	ORVOCs	3.85×10^{-11}
101	Hexanal	ORVOCs	2.88×10^{-11}
71	MACR	ORVOCs	2.86×10^{-11}
	MVK	ORVOCs	2.01×10^{-11}
155	1,8-Cineole[c]	oMT	2.26×10^{-11}
45	Acetaldehyde	ORVOCs	1.49×10^{-11}
107	o-Xylenes	ORVOCs	1.36×10^{-11}
153	Methyl salicylate[c]	ORVOCs	1.11×10^{-11}
	Camphor[c]	oMT	9.88×10^{-12}
93	Toluene	OVOCS	5.63×10^{-12}
47	Ethanol	OVOCS	3.21×10^{-12}
73	MEK	OVOCs	1.11×10^{-12}
33	Methanol	OVOCS	8.96×10^{-13}
61	Acetic acid	OVOCS	8.00×10^{-13}
59	Acetone	OVOCS	1.75×10^{-13}

Note. The k-rates are given for 298.15 K in units of cm^3 molecule^{-1} s^{-1}. The compounds are grouped by mass to charge ratio (*m/z*) and sorted by reactivity, distinguishing 3 different groups: high reactivity with OH *k*-rates > 1.0 x 10^{-10} (dark grey), medium high reactive VOCs (ORVOCs also including some oxygenated monoterpenes (oMTs), medium grey) with OH *k*-rates between 1.0 (0.988 in case of camphor) and 10 x 10^{-11}, and low reactive other VOCs (OVOCs, white background) with OH *k*-rates < 1.0 x 10^{-11}. If not separately indicated, the values were taken from the Master Chemical Mechanism, MCM v3.2 (Saunders et al., 2003), via website: http://mcm.york.ac.uk (last access: 01.07.2021).
[a]Peeters et al. (2007). [b]Hakola et al. (2012). [c]Values taken from ApoWin v1.92 module of the EPI software (www.epa.gov).

kgDW m^{-2} and 1.11 ± 0.09 kgDW m^{-2}, respectively), which was, however, not much different from the the overall biomass production of grass for the whole year (1.49 ± 0.05 kgDW m^{-2}). Different development stages have been recognized for different species such as reproductive growth, emerging inflorescences and flowering, fruit development and ripening. Only for ryegrass, development did continue beyond flowering as the cuts interrupted the post-flowering development. Gross primary production (GPP) followed temperature and PAR (see supplement Figure S4-S6 in Supporting Information S1). Drought stress cannot fully be excluded in late summer 2015 for maize, as well as for a short period in July 2016, but is unlikely for 2017 which was characterized by high precipitation.

The LandscapeDNDC model could well represent photosynthesis, as well as leaf and biomass development, particularly in the early developmental phases (Figure 1). In the late phases, carbon uptake seems to be slightly under- (maize) or overestimated (oil-seed rape), which might be related to underestimated drought (maize) and disregarded seasonal decline of enzymes (oil-seed rape).

3.2. BVOC Emissions

Daily mean BVOC fluxes can be accumulated for different periods as well as the whole observation (growing) period, which differ in length and flux magnitude (see Table 5). Highest mean values over the entire investigation period were generally observed for the green leaf volatiles (GLVs, mainly maize) and other (oxygenated) compounds with relatively low reactivity (i.e., methanol, ethanol, acetone, acetaldehyde, and acetic acid), which together contribute 73%, 99%, and 94% of all observed emissions for maize, oil-seed rape and ryegrass respectively. Methanol was particular dominant in oil-seed rape and ryegrass, contributing more than 80% of the whole year emissions on a molecular basis while it was still one of the two main compounds in maize. Terpenoids are emitted by all plants but contributed to major degrees only in maize.

Whereas emissions correlated well with temperature and leaf area throughout the season in general, BVOC emissions were significantly less sensitive in some periods than others. For maize, these different sensitivities have been previously attributed to the different phenological stages (Wiß et al., 2017). Now, this sensitivity seems to be compound-specific since for example, acetic acid increases its SEF during growth in oil-seed rape while the *SEFs* of acetaldehyde decrease. However, the impacts are not easily distinguished, since meteorological conditions and growth stages vary simultaneously, for example, the onset of flowering in oil-seed rape occurs in parallel with a substantial temperature and PAR increase.

Using compound-specific parameterization differentiated by plant species, BVOC emissions could generally be well reproduced (except in cases where large depositions occurred). Examples for all species are presented in Figure 2. These also demonstrate the impact of the before-mentioned sensitivity change between seasons or developmental stages, resulting for example, in an overestimation of monoterpene emissions from maize in late August 2015.

From the analysis of all different compounds, three emission groups were derived that differ in their reactivity (see Table 4). All simulated and measured compounds within one group were summed up for each species (Figures 3–5).
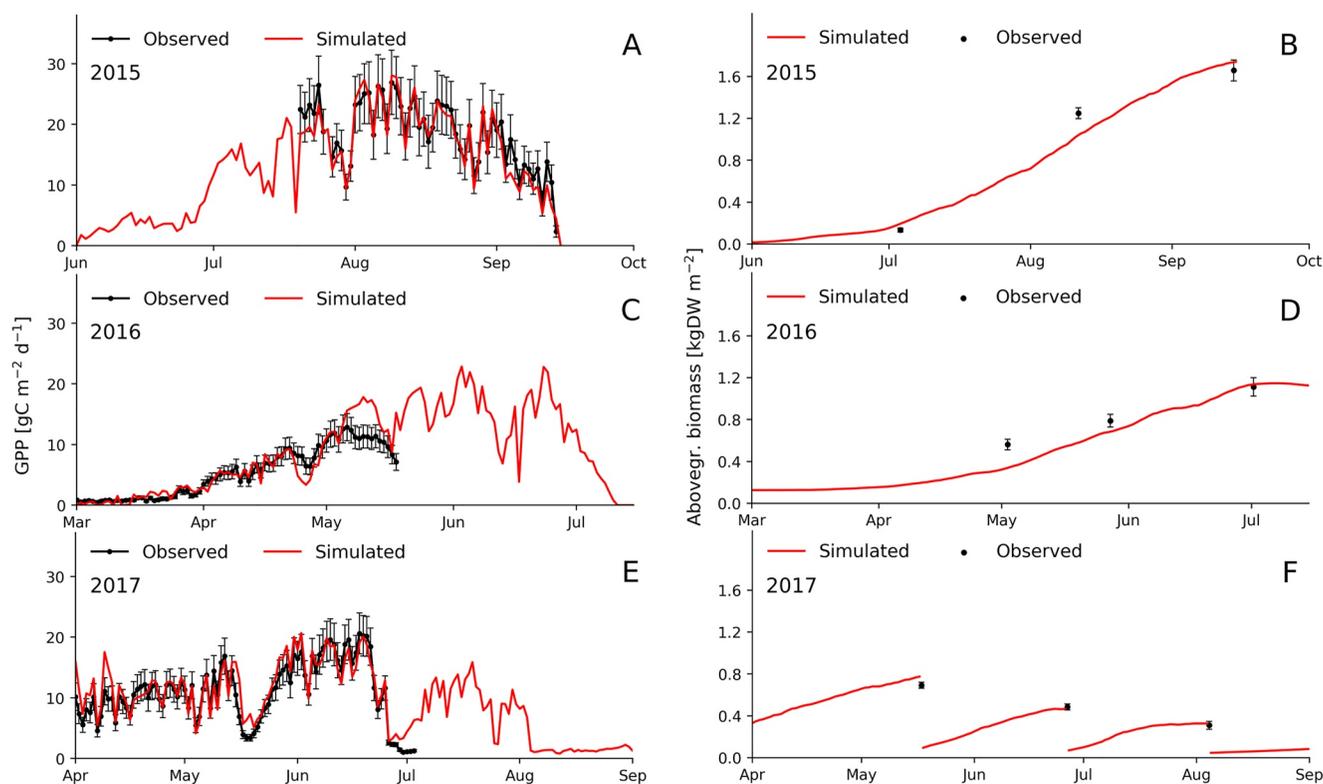
Figure 1. Gross primary production simulated and derived from measurements (a, c, e) as well as biomass development (b, d, F) for the three investigated crops: maize (a), (b), oil-seed rape (c), (d), and ryegrass (e), (f). Simulations are shown with red lines, observations are represented with black dots (Error bars indicate ± the standard error of the sum).

3.3. Rotation Cycle Comparisons

Simulations for three consecutive years have been carried out to support conclusions about average BVOC emissions and their dependence on inter-annual meteorological differences during a growing season (Figure 6). Regarding biomass and GPP development, slightly warmer spring periods in 2016 (intensive) and 2017 (moderate) led to an earlier onset of plant growth and also to an earlier growth cessation of about 1–2 weeks compared to 2015. It can be seen that drought limited crop growth only in 2016, where a severe precipitation deficit occurred in July, which particularly affected ryegrass development. Overall, the impact of interannual variation on growth is relatively small.

Regarding BVOC emissions, however, the differences in weather led to considerably higher variations. Generally, simulated emissions of each crop were the highest in 2015, which is mainly caused by the high temperature in August of +3°C above the long-term mean. In contrast, temperatures in 2016 were relatively high in June/July and September, periods in which the leaf area and thus the potential for BVOC emissions was reduced for maize (due to not fully developed foliage), oil-seed rape (due to early cutting before September) and ryegrass (due to previous cuttings and less growth in autumn). Table 6 presents simulated mean annual BVOC emissions rates and variabilities for all 3 years.

Generally, with 91.4 ± 8.0 mmol m^{-2}, cultivation of oil-seed rape lead to the highest amount of total BVOCs emission per year on a mole basis followed by ryegrass (15.7 ± 0.6 mmol m^{-2}) and maize (2.5 ± 0.1 mmol m^{-2}). Besides the variability and seasonality, the different composition of the blend is decisive for the potential impacts of BVOCs on air chemistry because all compounds have a different reactivity (see Table 4). The results of the weighting procedure indicate that in contrast to the huge variability of total annual BVOC emission fluxes (37-fold between oil-seed rape and maize, see supplement Figure S10-S12 in Supporting Information S1), the difference between the potential annual impact on air chemistry is relatively small (6-fold between oil-seed rape and ryegrass, see Figure 7). The highest impact on atmospheric chemistry is expected from oil-seed rape BVOC

Table 5
24-Hour Mean Molar BVOC Emissions for the Experimental Period in Pmol m⁻² Ground and s⁻¹ (Negative Fluxes Set to Zero) Including the Fraction of Each Compound to the Total BVOC Emission

Compound	Crop species	Period 1	%	Period 2	%	Whole period	%
Methanol	Maize	135	18	69.1	16	98.6	17
	Osr	900	92	3902	83	2438	85
	Ryegrass	1648	80	558	78	1417	80
Acetaldehyde	Maize	97.9	13	56.7	13	76.2	13
	Osr	18.0	1.8	118	2.5	68.9	2.4
	Ryegrass	185	9.0	58.5	8.2	158	8.9
Ethanol	Maize	12.6	1.7	16.4	3.8	14.6	2.5
	Osr	5.9	0.6	109	2.3	58.4	2.0
	Ryegrass	48.0	2.3	4.3	0.6	38.8	2.2
Acetone	Maize	95.4	13	71.1	17	83.1	14
	Osr	20.1	2.1	87.4	1.9	54.2	1.9
	Ryegrass	92.0	4.5	71.7	10	87.8	5.0
Acetic acid	Maize	n.d.		n.d.		n.d.	
	Osr	9.3	0.9	208	4.4	111	3.9
	Ryegrass	6.1	0.3	0.0	0.0	4.8	0.3
m/z 69	Maize	46.5	6.1	18.6	4.4	31.7	5.4
Isoprene	Osr	8.5	0.9	31.0	0.7	19.8	0.7
Isoprene	Ryegrass	17.2	0.8	8.2	1.1	15.3	0.9
m/z 71	Maize	23.7	3.1	14.1	3.3	18.6	3.2
MACR/MVK	Osr	2.8	0.3	24.0	0.5	13.6	0.5
MACR/MVK	Ryegrass	6.2	0.3	0.4	0.1	5.0	0.3
	Maize	n.d.		n.d.		n.d.	
m/z 73	Osr	3.5	0.4	40.6	0.9	22.4	0.8
MEK	Ryegrass	16.1	0.8	2.7	0.4	13.2	0.7
m/z 79	Maize	n.d.		n.d.		n.d.	
	Osr	0.7	0.1	10.7	0.2	5.8	0.2
	Ryegrass	n.d.		n.d.		n.d.	
Toluene	Maize	n.d.		n.d.		n.d.	
	Osr	0.5	0.0	10.4	0.2	5.6	0.2
	Ryegrass	n.d.		n.d.		n.d.	
Hexenal	Maize	34.1	4.5	26.5	6.2	30.4	5.2
	Osr	1.0	0.1	16.2	0.3	8.8	0.3
	Ryegrass	11.3	0.6	1.3	0.2	9.2	0.5
Hexanal	Maize	83.9	11	65.6	15.4	75.0	12
	Osr	3.2	0.3	76.3	1.6	40.6	1.4
	Ryegrass	13.0	0.6	0.7	0.1	10.4	0.6
Xylenes	Maize	9.6	1.3	9.3	2.2	9.5	1.6
	Osr	0.5	0.1	8.8	0.2	4.7	0.2
	Ryegrass	n.d.		n.d.		n.d.	
m/z 118	Maize	n.d.		n.d.		n.d.	
	Osr	0.2	0.0	14.3	0.3	7.4	0.3
	Ryegrass	n.d.		n.d.		n.d.	

Table 5
Continued

Compound	Crop species	Period 1	%	Period 2	%	Whole period	%
Limonene	Maize	132	17	48.4	11	88.1	15
Thujene; Myrcene; trans-β-Ocimene	Osr	0.4	0.0	24.6	0.5	12.8	0.4
Myrcene	Ryegrass	4.8	0.2	2.9	0.4	4.4	0.2
DMNT	Maize	17.1	2.2	10.2	2.4	13.6	2.3
	Osr	n.d.		n.d.		n.d.	
	Ryegrass	n.d.		n.d.		n.d.	
Camphor; MeSA; 4-Ethylguaiacol	Maize	36.5	4.8	9.6	2.2	22.2	3.8
	Osr	n.d.		n.d.		n.d.	
	Ryegrass	n.d.		n.d.		n.d.	
1,8-Cineole	Maize	9.3	1.2	4.4	1.0	6.8	1.2
	Osr	n.d.		n.d.		n.d.	
	Ryegrass	n.d.		n.d.		n.d.	
α-Humulene	Maize	28.4	3.7	5.7	1.3	16.4	2.8
Junipene	Osr	1.5	0.2	1.3	0.0	1.4	0.0
Isolongifolene	Ryegrass	2.5	0.1	4.4	0.6	2.9	0.2
Total	Maize	762	100	426	100	585	100
	Osr	976	100	4668	100	2866	100
	Ryegrass	2050	100	713	100	1766	100

Note. Period 1 and period 2 refer to flowering (24 days) and ripening (28 days) in maize, to inflorescence emergence (14 days) and flowering (4 days) in oil-seed rape (Osr), and to heading (19 days) and flowering (20 days) in ryegrass, respectively.

emissions (factor 2.4 larger than maize), which is followed by maize and ryegrass (only 40% that of maize). As the composition of BVOCs emitted from oil-seed rape is similar to that of ryegrass, the difference between their total emissions (5.8-fold) is similar to the difference of their relative impact on atmospheric reactivity (6.0-fold). In contrast, maize, emits relatively large amounts of terpenes (limonene, α-humulene) as well as the homoterpene DMNT, which are highly reactive. Thus, despite the relatively small amount of annual BVOC emissions compared to oil-seed rape and ryegrass (approximately 3% and 16% of the oil-seed rape and ryegrass emissions), the potential impact on air chemistry of maize is about 2.5-fold higher than that of ryegrass and only about 2.4-fold less than oil-seed rape.

4. Discussion and Conclusions

4.1. Comparison of Simulations With Field Measurements

From the comparison of simulations with measurements a couple of important points can be derived. First, it seems that particularly high reactive compounds tend to be underestimated at least during specific development phases (e.g., maize in the flowering phase (Period 1), Figure 3). This clearly indicates that a period-specific parametrization would be superior to the use of a whole-year emission parameter, particularly with respect to light-dependent and generally more reactive compounds than emissions from storages.

Second, some uncertainties regarding the absolute amount as well as the temporal variation of emissions may be related to BVOCs formed in or deposited to the soil. BVOC emissions from soil have been reported in many studies before (Peñuelas et al., 2014) but also deposition processes seem to be common and sometimes relevant in magnitude (Bachy et al., 2020; Spielmann et al., 2017). Emissions as well as consumption has been attributed to soil microorganisms, resulting in microbial activity and diversity being the main driver (Abis et al., 2020). These effects are influenced by agricultural management, which alters BVOC exchange through lagged effects (e.g., the previously planted crop) or the management of pests and diseases (Malone et al., 2020).
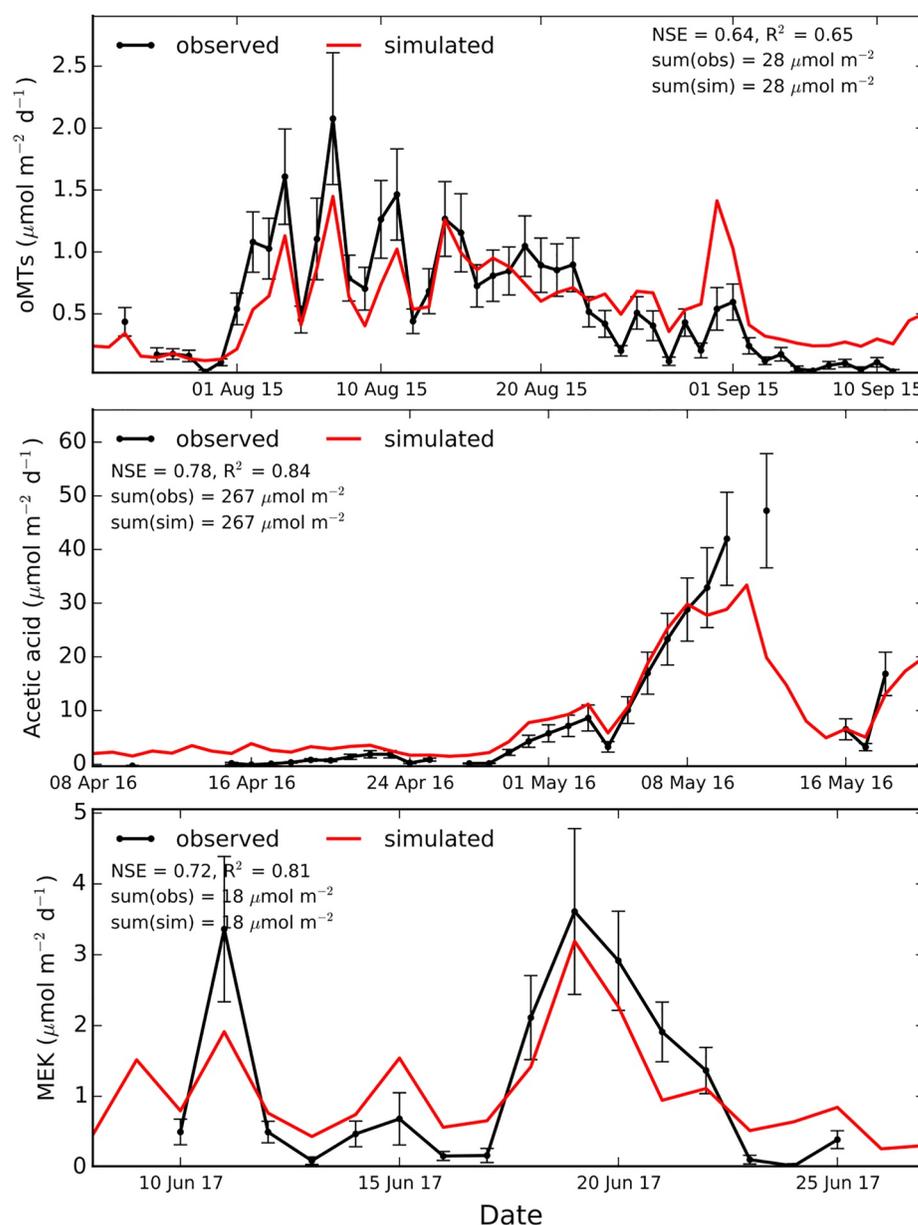
Figure 2. Examples of observed and simulated emissions for the specific crops (see complete results in the supplements Figure S7-S9 in Supporting Information S1). Top: oxygenated monoterpenes for maize (oMTs, mainly 1,8-Cineole); Middle: acetic acid for oil-seed rape; Bottom: methyl ethyl keton (MEK) for ryegrass. Simulations are shown with red lines, observations are represented with black dots (Error bars indicate ± the standard error of the sum).

Finally, for some specific compounds, that is, ethanol, methanol and (for ryegrass) acetic acid, the fit between simulations and measurements is very poor (Figure S7 in Supporting Information S1). These discrepancies are mostly explained by the water-solubility of the mentioned compounds, because during wet periods they are dissolved in the moisture at leaf or soil surfaces, which leads to reduced net emission rates or even negative emissions. The importance of this deposition process has thus been demonstrated with our measurements but is not yet considered in the model.

The results also demonstrate that at least for oil-seed rape and ryegrass, which can grow from late spring until early autumn, measurement periods did not cover the whole range of potential importance.
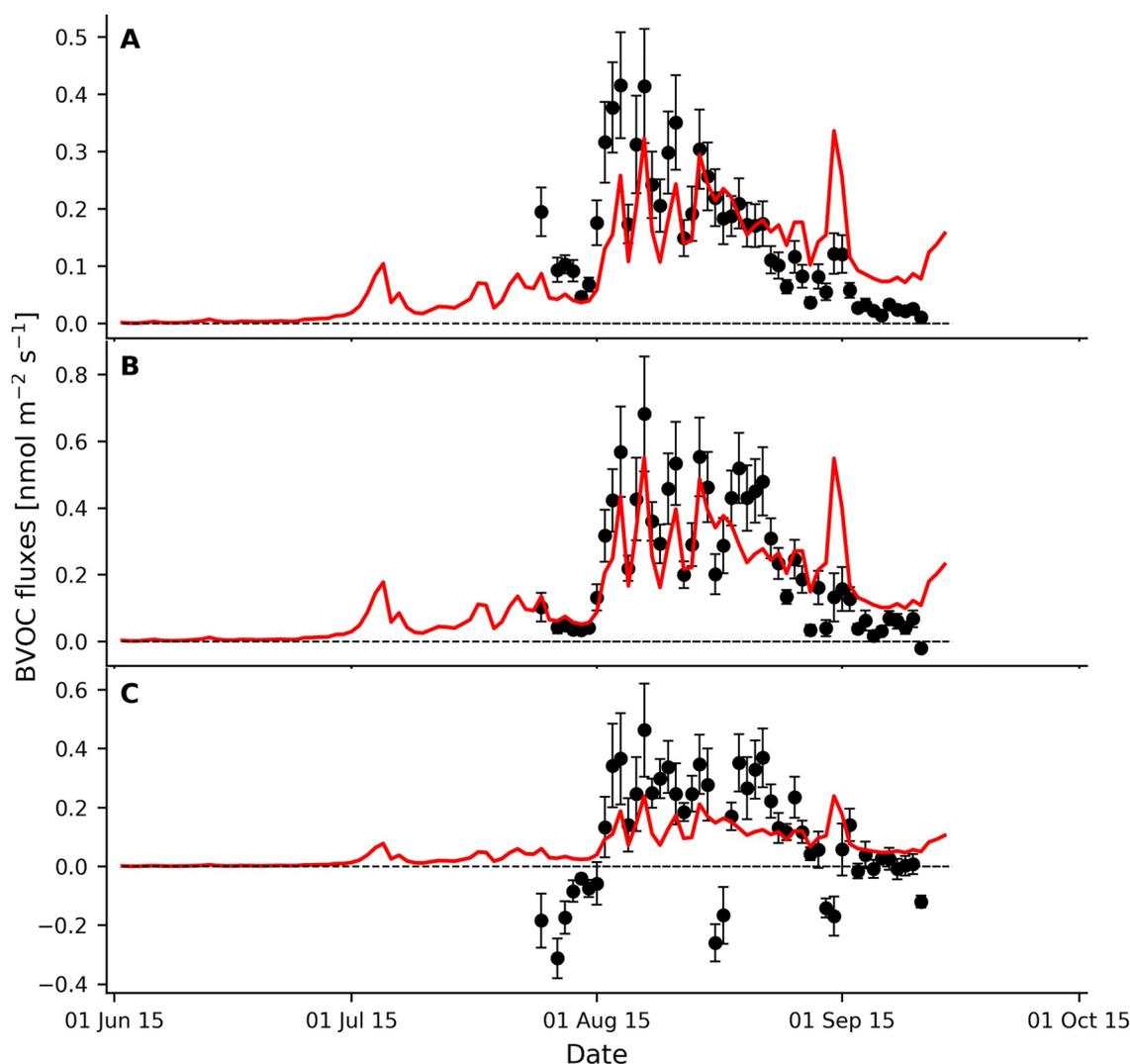
Figure 3. Measured (points with error bars) and simulated (lines) emissions pooled into (a) high, (b) medium, and (c) low reactivity classes (according to Table 4) for maize 2015.

4.2. Comparison With Other Emission Measurements

Several measurements of BVOC emissions have been presented in the literature for maize, some for oil-seed rape and only a few for ryegrass (see Table 7). For maize, the data indicate a particularly large variation of what compounds are emitted in which quantity, with the majority of publications indicating much larger net emissions of methanol (Das et al., 2013; Gonzaga Gomez et al., 2019; Graus et al., 2013; Mozaffar et al., 2018) than recorded in our field survey (Wiβ et al., 2017). In contrast, our measurements demonstrated larger fluxes of monoterpenes (see also Wiβ et al., 2017) than presented in most other investigations (Bachy et al., 2016; Graus et al., 2013; Street et al., 1997). Moreover, we herein demonstrate the emission of sesquiterpenes and oxygenated monoterpenes that have not been described in any of the field measurements before (although they have been recognized in laboratory experiments). In contrast to maize, our findings for oil-seed rape are rather at the upper range of previous field observations regarding methanol (Acton et al., 2018; Gonzaga Gomez et al., 2019) as well as GLV emissions (König et al., 1995). Notably, considerable net emissions of other oxygenated hydrocarbons such as of acetone, acetaldehyde, and ethanol were found that were only seldom reported before (Bsaibes et al., 2020; Gonzaga Gomez et al., 2019; McEwan & MacFarlane Smith, 1998). Terpenoid emissions in oil-seed rape were either higher (Bsaibes et al., 2020; Himanen et al., 2009; McEwan & MacFarlane Smith, 1998) or lower (König et al., 1995; Müller et al., 2002) than indicated by our observations, with one investigation that could not
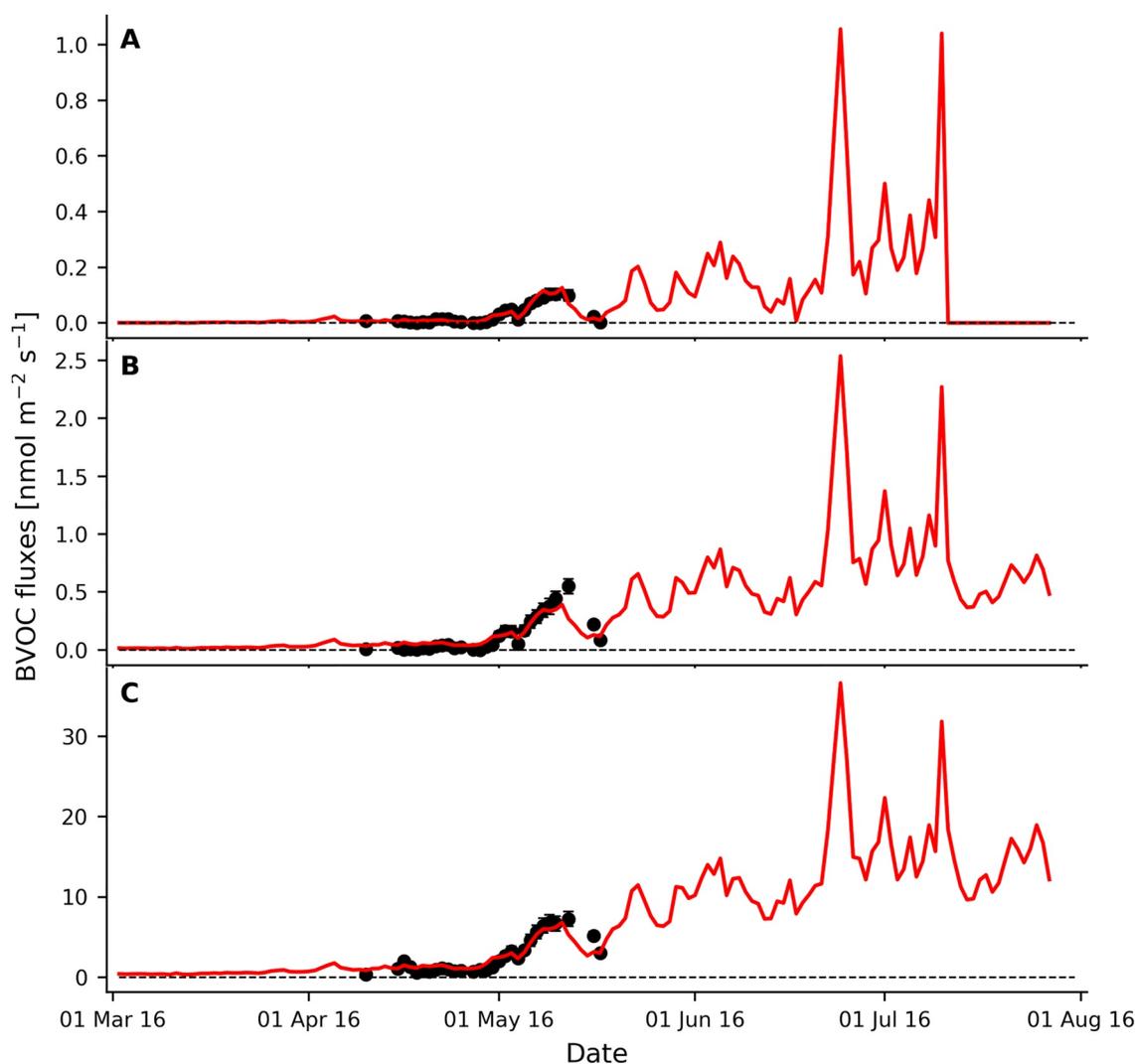
Figure 4. Measured (points with BVOC error bars) and simulated (lines) emissions pooled into (a) high, (b) medium, and (c) low reactivity classes (according to Table 4) for oil-seed rape 2016.

find any monoterpene emission at all (Morrison et al., 2016). Regarding ryegrass, we present the first comprehensive estimate of the BVOC emission spectrum that has been derived from field measurements. The few other investigations concentrated on OVOCs and indicated either no (Custer & Schade, 2007) or moderate net emission of methanol and acetaldehyde for *Lolium multiflorum* (Kirstine et al., 1998). Laboratory investigations indicated furthermore high emissions of GLVs and sesquiterpenes as well as emissions of monoterpenes and oxygenated monoterpenes (Pańka et al., 2013), which however, seem to play only a minor or no role under field conditions.

We hypothesize that these differences may at least partly be due to too short measurement periods that do not include deposition (because measurements took place under favorable weather conditions). Estimations based on such measurements would thus be prone to overestimate in particular emission of compounds that are water-soluble such as methanol and ethanol (Das et al., 2013; Gonzaga Gomez et al., 2019). In some occasions, plants may have been in early or late developmental stages that were not representative for whole-season emissions. Also, it should be noted that measurements at single leaves or small plants may be considerably biased if ecosystem fluxes shall be derived (Graus et al., 2013). Likely, some of the differences measured herein may also be due to the use of different cultivars or the presences of undetected stressors. For example, insect infestation has increased GLVs (Christensen et al., 2013), fungal infections are known to induce alcohols (Usseglio et al., 2017), while various stressors were connected to elevated terpenoid emissions (Block et al., 2019; M. Chiriboga. et al., 2018).
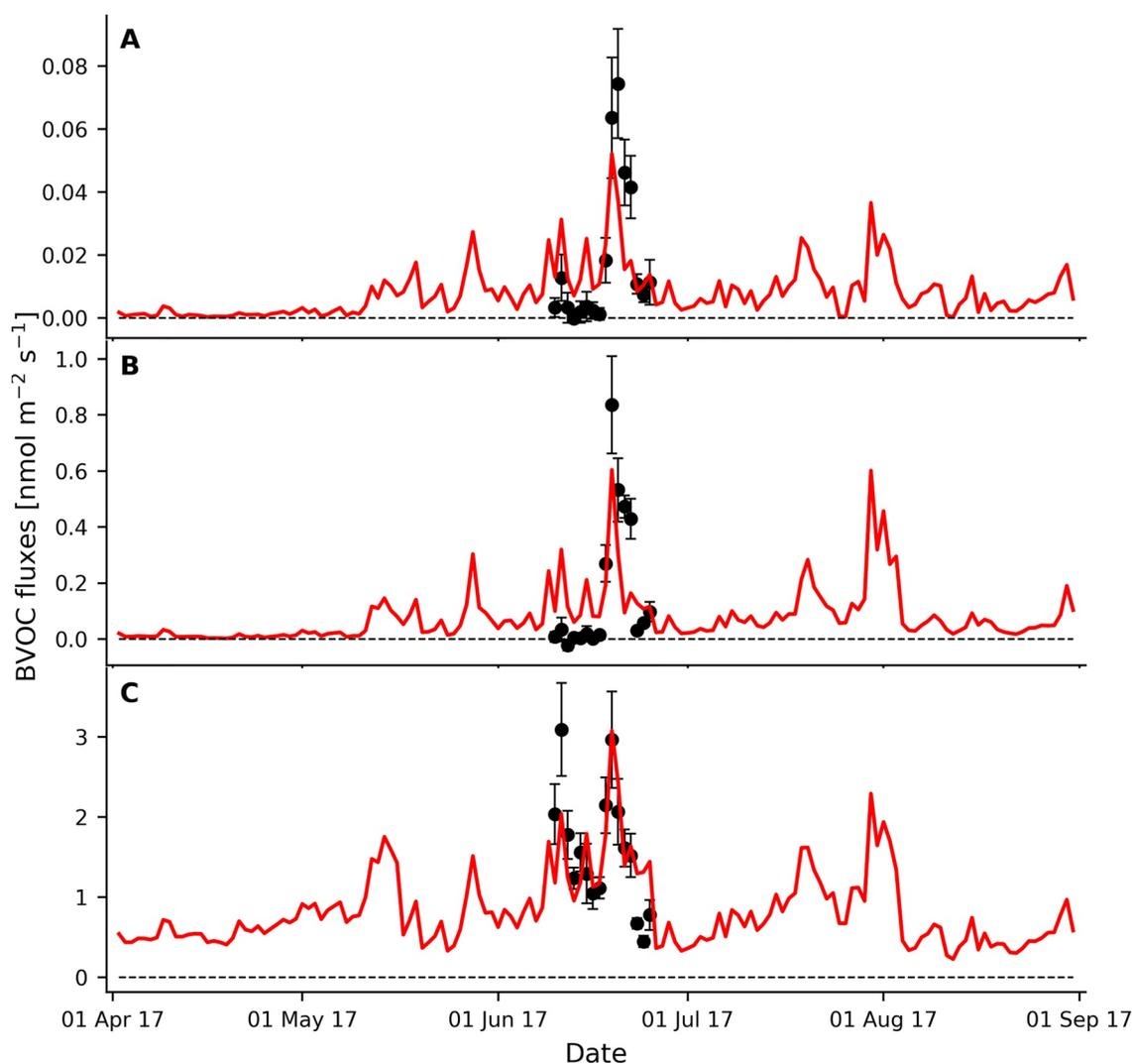
Figure 5. Measured (points with error bars) and simulated (lines) pooled into (a) high, (b) medium, and (c) low reactivity classes (according to Table 4) for ryegrass 2017.

It should also be noted that by using large, canopy chambers, all plant-atmosphere exchanges including BVOC emissions are derived at the whole ecosystem level, including trace gas exchange from the soil.

4.3. Importance for Atmospheric Chemistry

Cropland emission inventories have been built with and without differentiation of crop types and species using quite different SEFs (see Table 7). In most cases, croplands are not considered at all (pooled into grassland species), while sometimes fixed SEFs for cropland (usually non-irrigated) are assumed that are scaled with a fixed (average; Zheng et al., 2010) or regionally differentiated, for example, based on satellite images, biomass value per area (Gulden & Yang, 2006; Li et al., 2018). The fixed SEFs and leaf biomass densities, however, lump together crop species with very different emission pattern, for example, emitting or not emitting isoprene. While the average emission parameters may be correct under a specific condition, such inventories cannot account for changes in crop abundance, as for example, expanding cannabis plantations (Wang et al., 2019) or the continuous increase in maize covered area in Europe (see introduction). In contrast, inventories based on species-specific parameterization of BVOC emissions as well as foliage biomass density can be easily updated with agricultural statistics. For example, the cropland parameterization from the latest inventory of Europe (Karl et al., 2009) largely overestimates emissions of all compound classes when compared with the three species investigated
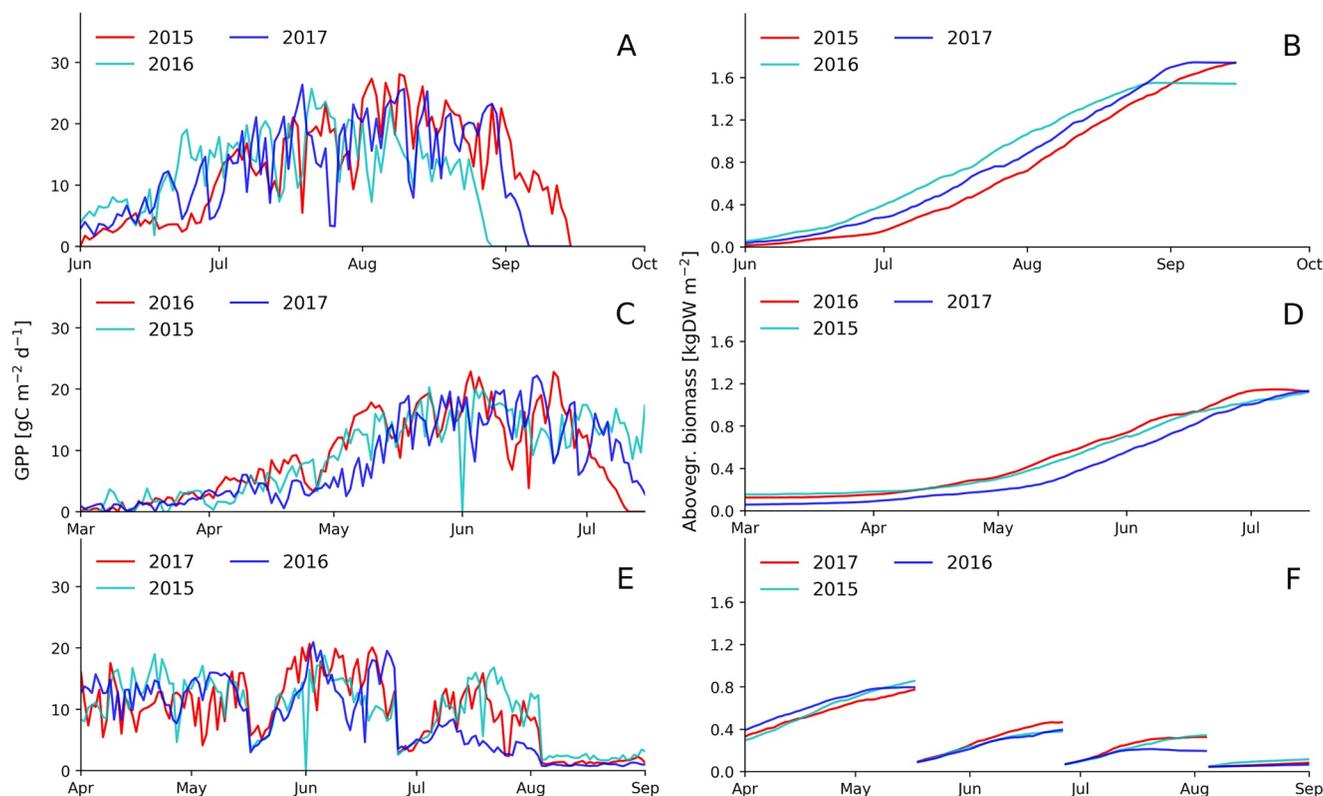
Figure 6. Simulated Gross Primary Production (a, c, e) and biomass development (b, d, f) for the three investigated crops maize (a), (b), oil-seed rape (c), (d), and ryegrass (e), (f) for all three investigated years.

here. The difference would be even more severe for other low emitting crop species which have been found in various genera of energy crops such as *Miscanthus* or *Panicum* (Copeland et al., 2012; Hu et al., 2018; Morrison et al., 2016), while planting strong isoprene emitters such as giant cane (*Arundo donax*; Porter et al., 2012) or bamboo (*Phyllostachys* spp; Okumura et al., 2018) would result in an underestimation of BVOC emission fluxes.

Overall, we show that total as well as compound-specific BVOC emissions from bioenergy crops can well be represented using the principal mechanisms of the JJv model that integrates phenological and physiological responses on environmental conditions. The model enables to represent leaf expansion and the development of specific ripening stages which results in large and realistic seasonal variations in BVOC emission rates and patterns. Thus, a highly spatial and temporal resolved inventory might be feasible provided that emission parameters for the major species are available. Nevertheless, some deviations between simulations and observations (mean $\pm$ standard deviation of NSE of 0.48 ± 0.09, 0.84 ± 0.08, and 0.47 ± 0.18, for maize, oil-seed rape, and ryegrass respectively for all simulated BVOC emissions) indicate that modeling would still profit from a dynamic seasonality effect that accounts for plant developmental stages such as flowering. How to consider such an effect is still an open discussion. A simple temperature and light dependency that had been developed particularly for woody species (Guenther et al., 2006) has been applied also for crops (Karl et al., 2009) but its suitability for species that shift into different development stages remains to be shown. In conjunction with a seasonally realistic agricultural rotation management (i.e., sowing and harvesting) also spatial variation can be reasonably covered.

Finally, the conversion of BVOC emissions into reactivity has shown that not only the emission strength of individual compounds but also the emission pattern and the individual (or group) reactivity of the compounds need to be considered. This has recently also been postulated for a short-term experiment at an oil-seed rape field in France (Bsaibes et al., 2020). In particular compounds with very high OH-reactivities can determine air chemistry in specific periods. The ability of emitting such reactive compounds, however, is very differently expressed in different agricultural species, but this species-dependence is generally not differentiated in regional air chemistry calculations (Chatani et al., 2015; Kim et al., 2017; Poupkou et al., 2009). For example, significant emissions of

Table 6
Simulated Mean Annual BVOC Emission Rates (μmol m⁻² a⁻¹) From Maize, Oil-Seed Rape, and Ryegrass Measured From 2015 to 2017 at the CarboZALF Field Site in Dedelow (SD Denotes the Standard Deviation Relative to the Number of Measurements Indicated in Table 1)

Compound Hemiterpenes	Maize	Mean SD	Oil-seed rape	Mean SD	Ryegrass	Mean SD
Isoprene	0	0	669	131	110	19
Monoterpenes (and oMTs)						
Limonene	454	53	0	0	0	0
Myrcene	0	0	415	81	27.9	4.8
(Camphor)	110	15	0	0	0	0
(1,8-Cineole)	34.0	4.5	0	0	0	0
all MTs	*598*		*415*		*27.9*	
Homoterpenes						
DMNT	69.2	7.8	0	0	0	0
Sesquiterpenes						
alpha-Humulene	82.0	11	0	0	0	0
Other VOCs						
Acetaldehyde	378	44	2047	210	1174	125
Acetic acid	0	0	3704	588	0	0
Acetone	429	49	1736	208	704	73
Ethanol	0	0	1917	374	277	47
Hexanal	374	48	1407	201	67.0	11
Hexenal	149	19	254	50	54.9	9.4
m/z 69	164	19	0	0	0	0
m/z 71	79.3	12	0	0	0	0
m/z 73	0	0	767	118	0	0
m/z 79	0	0	175	34	0	0
m/z 118	0	0	242	47	0	0
MACR/MVK	0	0	444	66	9.7	1.7
MEK	0	0	0	0	98.0	17
Methanol	93.6	17	77221	7925	13220	627
Toluene	0	0	180	35	0	0
Xylenes	48.8	5.5	150	29	0	0
All other VOCs	*1715*		*90244*		*15605*	
Total	2465	105	91329	7967	15743	646

limonene, DMNT and sesquiterpenes have been found solely in maize, while in ryegrass only small amounts of isoprene were emitted, rendering this species as low-impact to air chemistry despite its relatively large emissions of other oxygenated compounds. In this regard, it should be noted that within the same chemical class, reactivities can differ by almost two orders of magnitude (see Table 4). This leads to the fact that a low xylene emission in maize approximately compensates the OH reactivity of the very high acetic acid emissions in oil-seed rape. The presented research demonstrates that compounds with small quantitative contributions do significantly affect air chemistry. Even if the molar amount of emissions is one order of magnitude different between each reactivity group (oil-seed rape and ryegrass), the importance for air chemistry is in the same range since also the reactivity difference is about one order of magnitude.
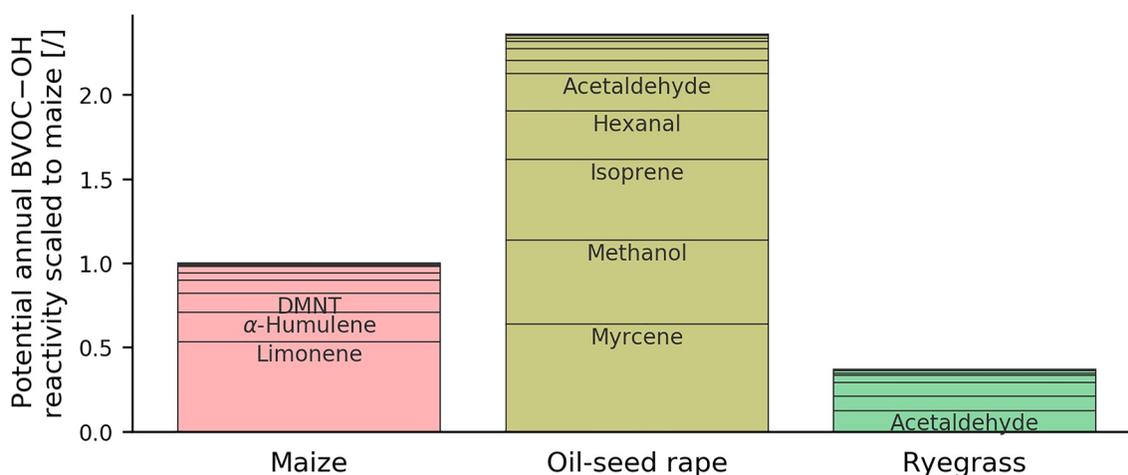
Figure 7. Potential mean annual BVOC-OH reactivity from maize, oil-seed rape, and ryegrass based on the 3 years of the investigation period. All values are scaled to the reactivity of maize. Only compounds with contribution >0.1 are considered.

In order to derive more general and responsive simulations that are able to potentially cover interannual as well as decadal trends and are applicable on a regional scale, species-specific emission strength as well as compositions should therefore be considered. Finally, the full year simulations reveal that the variability of emissions during the year is high for all crops and that single days or short periods can have disproportional large impacts on air chemistry.

Table 7
Overview of Terpenoid BVOC Standard Emission Factors (SEF) From Maize, Oil-Seed Rape, and Ryegrass Compared With Standard Cropland Emissions Used in Regional Models

Vegetation type	Biomass density	SEF isoprene	SEF monoterpenes	SEF Sesqui-terpenes (ORVOCs)	SEF OVOCs	Reference
Oil-seed rape	600	0.22 0.45	0.4	0	11.53	This study
			0.56			
	800	0	0.1	-	0.3	Simon et al. (2006)
	400	0	1	0.1	2	Karl et al. (2009)
	-	0	0.04	0	0.06	König et al. (1995)
Ryegrass	400	0.11	0.08	0	3.69	This study
		0.10	0.05			
	1600	0	0	-	0.4	Simon et al. (2006) [a]
Maize	1200	0	0.19	0.06	0.27	This study
			0.16	0.05		
	1610	0	1	0.1	2	Karl et al. (2009)
	1610	0	0.11	-	1	Simon et al. (2006)
	1610	0	0.22	-	0.88	Lamb et al. (1993)
	1610	0.5	0	-	0	Pierce et al. (1998)
Non-irrigated cropland	520–800	0.5	1	0.1	2	Karl et al. (2009)
	satellite derived	0.1	0.25	-	0.15	Li et al. (2018)
	740	0.01	0.03	-	0.02	Zheng et al. (2010)
	satellite derived	0	0.1	1	1	Levis et al. (2003)
	1000	0	0.1	-	-	Simpson et al. (1999)

Note. In order to provide this comparison, calculated emission obtained in this study were scaled to a photosynthetic photon flux density (PPFD) of 1000 µmol m^{-2} s^{-1} and 30°C in units of µg compound g^{-1} DW h^{-1}. The dry weight of leaf or plant biomass density used for scaling is also given in g m^{-2}.
[a]based on Kirstine et al. (1998).

Data Availability Statement

All measured and simulated emission data are provided in the supplement as figures. All data are permanently and freely accessible in the Radar4KIT repository (https://doi.org/10.35097/561).

References

Abeleira, A., Pollack, I. B., Sive, B., Zhou, Y., Fischer, E. V., & Farmer, D. K. (2017). Source characterization of volatile organic compounds in the Colorado Northern Front Range metropolitan area during spring and summer 2015. *Journal of Geophysical Research: Atmospheres*, *122*(6), 3595–3613. https://doi.org/10.1002/2016jd026227

Abis, L., Loubet, B., Ciuraru, R., Lafouge, F., Houot, S., Nowak, V., et al. (2020). Reduced microbial diversity induces larger volatile organic compound emissions from soils. *Scientific Reports*, *10*(1), 6104. https://doi.org/10.1038/s41598-020-63091-8

Acton, W. J. F., Jud, W., Ghirardo, A., Wohlfahrt, G., Hewitt, C. N., Taylor, J. E., et al. (2018). The effect of ozone fumigation on the biogenic volatile organic compounds (BVOCs) emitted from *Brassica napus* above- and below-ground. *PLoS ONE*, *13*(12), e0208825. https://doi.org/10.1371/journal.pone.0208825

Ainsworth, E. A., & Rogers, A. (2007). The response of photosynthesis and stomatal conductance to rising [CO_2]: Mechanisms and environmental interactions. *Plant, Cell and Environment*, *30*(3), 258–270. https://doi.org/10.1111/j.1365-3040.2007.01641.x

Atkinson, R. (2000). Atmospheric chemistry of VOCs and NOx. *Atmospheric Environment*, *34*(12), 2063–2101. https://doi.org/10.1016/S1352-2310(99)00460-4

Bachy, A., Aubinet, M., Amelynck, C., Schoon, N., Bodson, B., Delaplace, P., et al. (2020). Dynamics and mechanisms of volatile organic compound exchanges in a winter wheat field. *Atmospheric Environment*, *221*, 117105. https://doi.org/10.1016/j.atmosenv.2019.117105

Bachy, A., Aubinet, M., Schoon, N., Amelynck, C., Bodson, B., Moureaux, C., et al. (2016). Are BVOC exchanges in agricultural ecosystems overestimated? Insights from fluxes measured in a maize field over a whole growing season. *Atmospheric Chemistry and Physics*, *16*(8), 5343–5356. https://doi.org/10.5194/acp-16-5343-2016

Bentsen, N. S., & Felby, C. (2012). Biomass for energy in the European Union - A review of bioenergy resource assessments. *Biotechnology for Biofuels*, *5*, 1–25. https://doi.org/10.1186/1754-6834-5-25

Bernacchi, C. J., Portis, A. R., Nakano, H., von Caemmerer, S., & Long, S. P. (2002). Temperature response of mesophyll conductance. Implications for the determination of Rubisco enzyme kinetics and for limitations to photosynthesis in vivo. *Plant Physiology*, *130*(4), 1992–1998. https://doi.org/10.1104/pp.008250

Bernacchi, C. J., Singsaas, E. L., Pimentel, C., Portis, A. R., & Long, S. P. (2001). Improved temperature response functions for models of Rubisco-limited photosynthesis. *Plant, Cell and Environment*, *24*, 253–259. https://doi.org/10.1111/j.1365-3040.2001.00668.x

Block, A. K., Vaughan, M. M., Schmelz, E. A., & Christensen, S. A. (2019). Biosynthesis and function of terpenoid defense compounds in maize (*Zea mays*). *Planta*, *249*(1), 21–30. https://doi.org/10.1007/s00425-018-2999-2

Brilli, F., Loreto, F., & Baccelli, I. (2019). Exploiting plant volatile organic compounds (VOCs) in agriculture to improve sustainable defense strategies and productivity of crops. *Frontiers of Plant Science*, *10*, 264. https://doi.org/10.3389/fpls.2019.00264

Bsaibes, S., Gros, V., Truong, F., Boissard, C., Baisnée, D., Sarda-Esteve, R., et al. (2020). Characterization of total OH reactivity in a rapeseed field: Results from the COV3ER experiment in April 2017. *Atmosphere*, *11*(3), 261. https://doi.org/10.3390/atmos11030261

Calfapietra, C., Fares, S., Manes, F., Morani, A., Sgrigna, G., & Loreto, F. (2013). Role of biogenic volatile organic compounds (BVOC) emitted by urban trees on ozone concentration in cities: A review. *Environmental Pollution*, *183*, 71–80. https://doi.org/10.1016/j.envpol.2013.03.012

Carslaw, K. S., Lee, L. A., Reddington, C. L., Pringle, K. J., Rap, A., Forster, P. M., et al. (2013). Large contribution of natural aerosols to uncertainty in indirect forcing. *Nature*, *503*(7474), 67–71. https://doi.org/10.1038/nature12674

Chatani, S., Matsunaga, S. N., & Nakatsuka, S. (2015). Estimate of biogenic VOC emissions in Japan and their effects on photochemical formation of ambient ozone and secondary organic aerosol. *Atmospheric Environment*, *120*, 38–50. https://doi.org/10.1016/j.atmosenv.2015.08.086

Chiriboga, M. X., Guo, H., Campos-Herrera, R., Röder, G., Imperiali, N., Keel, C., et al. (2018). Root-colonizing bacteria enhance the levels of (E)-β-caryophyllene produced by maize roots in response to rootworm feeding. *Oecologia*, *187*(2), 459–468. https://doi.org/10.1007/s00442-017-4055-5

Christensen, S. A., Nemchenko, A., Borrego, E., Murray, I., Sobhy, I. S., Bosak, L., et al. (2013). The maize lipoxygenase, ZmLOX10, mediates green leaf volatile, jasmonate and herbivore-induced plant volatile production for defense against insect attack. *The Plant Journal*, *74*(1), 59–73. https://doi.org/10.1111/tpj.12101

Copeland, N., Cape, J. N., & Heal, M. R. (2012). Volatile organic compound emissions from *Miscanthus* and short rotation coppice willow bioenergy crops. *Atmospheric Environment*, *60*, 327–335. https://doi.org/10.1016/j.atmosenv.2012.06.065

Courtois, E. A., Paine, C. E. T., Blandinieres, P.-A., Stien, D., Bessiere, J.-M., Houel, E., et al. (2009). Diversity of the volatile organic compounds emitted by 55 species of tropical trees: A survey in French Guiana. *Journal of Chemical Ecology*, *35*(11), 1349–1362. https://doi.org/10.1007/s10886-009-9718-1

Custer, T., & Schade, G. (2007). Methanol and acetaldehyde fluxes over ryegrass. *Tellus Series B Chemical and Physical Meteorology*, *59*(4), 673–684. https://doi.org/10.1111/j.1600-0889.2007.00294.x

Das, A. J., Stephenson, N. L., Flint, A., Das, T., & van Mantgem, P. J. (2013). Climatic correlates of tree mortality in water- and energy-limited forests. *PLoS ONE*, *8*(7), e69917. https://doi.org/10.1371/journal.pone.0069917

Dekker, J. H., & Sharkey, T. D. (1992). Regulation of photosynthesis in triazine-resistant and -susceptible *Brassica napus*. *Plant Physiology*, *98*(3), 1069–1073. https://doi.org/10.1104/pp.98.3.1069

Dominutti, P., Keita, S., Bahino, J., Colomb, A., Liousse, C., Yoboué, V., et al. (2019). Anthropogenic VOCs in Abidjan, southern west Africa: From source quantification to atmospheric impacts. *Atmospheric Chemistry and Physics*, *19*(18), 11721–11741. https://doi.org/10.5194/acp-19-11721-2019

Farquhar, G. D., Von Caemmerer, S., & Berry, J. A. (1980). A biochemical model of photosynthetic CO_2 assimilation in leaves of C_3 species. *Planta*, *149*, 78–90. https://doi.org/10.1007/BF00386231

Gelfand, I., Hamilton, S. K., Kravchenko, A. N., Jackson, R. D., Thelen, K. D., & Robertson, G. P. (2020). Empirical evidence for the potential climate benefits of decarbonizing light vehicle transport in the U.S. With bioenergy from purpose-grown biomass with and without BECCS. *Environmental Science & Technology*, *54*(5), 2961–2974. https://doi.org/10.1021/acs.est.9b07019

Ghirardo, A., Xie, J., Zheng, X., Wang, Y., Grote, R., Block, K., et al. (2016). Urban stress-induced biogenic VOC emissions and SOA-forming potentials in Beijing. *Atmospheric Chemistry and Physics*, *16*, 2901–2920. https://doi.org/10.5194/acp-16-2901-2016

Gonzaga Gomez, L., Loubet, B., Lafouge, F., Ciuraru, R., Buysse, P., Durand, B., et al. (2019). Comparative study of biogenic volatile organic compounds fluxes by wheat, maize and rapeseed with dynamic chambers over a short period in northern France. *Atmospheric Environment*, *214*, 116855. https://doi.org/10.1016/j.atmosenv.2019.116855

Graus, M., Eller, A. S. D., Fall, R., Yuan, B., Qian, Y., Westra, P., et al. (2013). Biosphere-atmosphere exchange of volatile organic compounds over C4 biofuel crops. *Atmospheric Environment*, *66*, 161–168. https://doi.org/10.1016/j.atmosenv.2011.12.042

Groenendijk, M., Dolman, A. J., van der Molen, M. K., Leuning, R., Arneth, A., Delpierre, N., et al. (2011). Assessing parameter variability in a photosynthesis model within and between plant functional types using global Fluxnet eddy covariance data. *Agricultural and Forest Meteorology*, *151*(1), 22–38. https://doi.org/10.1016/j.agrformet.2010.08.013

Grote, R. (2019). *Environmental impacts on biogenic emissions of volatile organic compounds (VOCs)* (p. 102). Final Report Rep. UmweltbundesamtDessau-Roßlau.

Grote, R., Morfopoulos, C., Niinemets, Ü., Sun, Z., Keenan, T. F., Pacifico, F., et al. (2014). A fully integrated isoprenoid emissions model coupling emissions to photosynthetic characteristics. *Plant, Cell and Environment*, *37*, 1965–1980. https://doi.org/10.1111/pce.12326

Gu, D., Guenther, A. B., Shilling, J. E., Yu, H., Huang, M., Zhao, C., et al. (2017). Airborne observations reveal elevational gradient in tropical forest isoprene emissions. *Nature Communications*, *8*, 15541. https://doi.org/10.1038/ncomms15541

Guenther, A., Karl, T., Harley, P., Wiedinmyer, C., Palmer, P. I., & Geron, C. (2006). Estimates of global terrestrial isoprene emissions using MEGAN (model of emissions of gases and aerosols from nature). *Atmospheric Chemistry and Physics*, *6*, 3181–3210. https://doi.org/10.5194/acp-6-3181-2006

Guenther, A., Zimmerman, P., Harley, P., Monson, R., & Fall, R. (1993). Isoprene and monoterpene emission rate variability: Model evaluations and sensitivity analysis. *Journal of Geophysical Research*, *98*(D7), 12609–12617. https://doi.org/10.1029/93JD00527

Gulden, L., & Yang, Z.-L. (2006). Development of species-based, regional emission capacities for simulation of biogenic volatile organic compound emissions in land-surface models: An example from Texas, USA. *Atmospheric Environment*, *40*, 1464–1479. https://doi.org/10.1016/j.atmosenv.2005.10.046

Haas, E., Klatt, S., Fröhlich, A., Werner, C., Kiese, R., Grote, R., et al. (2013). LandscapeDNDC: A process model for simulation of biosphere-atmosphere-hydrosphere exchange processes at site and regional scale. *Landscape Ecology*, *28*(4), 615–636. https://doi.org/10.1007/s10980-012-9772-x

Hakola, H., Hellén, H., Hemmilä, M., Rinne, J., & Kulmala, M. (2012). In situ measurements of volatile organic compounds in a boreal forest. *Atmospheric Chemistry and Physics*, *12*(23), 11665–11678. https://doi.org/10.5194/acp-12-11665-2012

Hakola, H., Tarvainen, V., Praplan, A. P., Jaars, K., Hemmilä, M., Kulmala, M., et al. (2017). Terpenoid and carbonyl emissions from Norway spruce in Finland during the growing season. *Atmospheric Chemistry and Physics*, *17*, 3357–3370. https://doi.org/10.5194/acp-17-3357-2017

Halliday, H. S., Thompson, A. M., Kollonige, D. W., & Martins, D. K. (2015). Reactivity and temporal variability of volatile organic compounds in the Baltimore/DC region in July 2011. *Journal of Atmospheric Chemistry*, *72*(3–4), 197–213. https://doi.org/10.1007/s10874-015-9306-4

Heald, C. L., & Kroll, J. H. (2020). The fuel of atmospheric chemistry: Toward a complete description of reactive organic carbon. *Science Advances*, *6*(6), eaay8967. https://doi.org/10.1126/sciadv.aay8967

Himanen, S. J., Nerg, A. M., Nissinen, A., Pinto, D. M., Stewart, C. N., Poppy, G. M., et al. (2009). Effects of elevated carbon dioxide and ozone on volatile terpenoid emissions and multitrophic communication of transgenic insecticidal oilseed rape (*Brassica napus*). *New Phytologist*, *181*(1), 174–186. https://doi.org/10.1111/j.1469-8137.2008.02646.x

Hoffmann, M., Jurisch, N., Albiac Borraz, E., Hagemann, U., Drösler, M., Sommer, M., et al. (2015). Automated modeling of ecosystem CO_2 fluxes based on periodic closed chamber measurements: A standardized conceptual and practical approach. *Agricultural and Forest Meteorology*, *200*, 30–45. https://doi.org/10.1016/j.agrformet.2014.09.005

Hoffmann, M., Jurisch, N., Garcia Alba, J., Albiac Borraz, E., Schmidt, M., Huth, V., et al. (2017). Detecting small-scale spatial heterogeneity and temporal dynamics of soil organic carbon (SOC) stocks: A comparison between automatic chamber-derived C budgets and repeated soil inventories. *Biogeosciences*, *14*(4), 1003–1019. https://doi.org/10.5194/bg-14-1003-2017

Holopainen, J. K., Kivimäenpää, M., & Nizkorodov, S. A. (2017). Plant-derived secondary organic material in the air and ecosystems. *Trends in Plant Science*, *22*(9), 744–753. https://doi.org/10.1016/j.tplants.2017.07.004

Holst, J., Grote, R., Offermann, C., Ferrio, J. P., Gessler, A., Mayer, H., et al. (2010). Water fluxes within beech stands in complex terrain. *International Journal of Biometeorology*, *54*, 23–36. https://doi.org/10.1007/s00484-009-0248-x

Hu, B., Jarosch, A. M., Gauder, M., Graeff-Hönninger, S., Schnitzler, J.-P., Grote, R., et al. (2018). VOC emissions and carbon balance of two bioenergy plantations in response to nitrogen fertilization: A comparison of *Miscanthus* and *salix*. *Environmental Pollution*, *237*, 205–217. https://doi.org/10.1016/j.envpol.2018.02.034

Kaplan, J. O., Folberth, G., & Hauglustaine, D. A. (2006). Role of methane and biogenic volatile organic compound sources in late glacial and Holocene fluctuations of atmospheric methane concentrations. *Global Biogeochemical Cycles*, *20*(2), GB2016. https://doi.org/10.1029/2005GB002590

Karl, M., Guenther, A., Köble, R., Leip, A., & Seufert, G. (2009). A new European plant-specific emission inventory of biogenic volatile organic compounds for use in atmospheric transport models. *Biogeosciences*, *6*(6), 1059–1087. https://doi.org/10.5194/bg-6-1059-2009

Kim, E., Kim, B.-U., Kim, H., & Kim, S. (2017). The variability of ozone sensitivity to anthropogenic emissions with biogenic emissions modeled by MEGAN and BEIS3. *Atmosphere*, *8*(10), 187. https://doi.org/10.3390/atmos8100187

Kirstine, W., Galbally, I., Ye, Y., & Hooper, M. (1998). Emissions of volatile organic compounds (primarily oxygenated species) from pasture. *Journal of Geophysical Research*, *103*(D9), 10605–10619. https://doi.org/10.1029/97JD03753

König, G., Brunda, M., Puxbaum, H., Hewitt, C. N., Duckham, S. C., & Rudolph, J. (1995). Relative contribution of oxygenated hydrocarbons to the total biogenic VOC emissions of selected mid-European agricultural and natural plant species. *Atmospheric Environment*, *29*(8), 861–874. https://doi.org/10.1016/1352-2310(95)00026-U

Kraus, D., Weller, S., Klatt, S., Santabárbara, I., Haas, E., Wassmann, R., et al. (2016). How well can we assess impacts of agricultural land management changes on the total greenhouse gas balance (CO_2, CH_4 and N_2O) of tropical rice-cropping systems with a biogeochemical model? *Agriculture, Ecosystems & Environment*, *224*, 104–115. https://doi.org/10.1016/j.agee.2016.03.037

Lamb, B., Gay, D., Westberg, H., & Pierce, T. (1993). A biogenic hydrocarbon emission inventory for the U.S. using a simple forest canopy model. *Atmospheric Environment*, *27*, 1673–1690. https://doi.org/10.1016/0960-1686(93)90230-V

Leuning, R. (1995). A critical appraisal of a combined stomatal-photosynthesis model for C3 plants. *Plant, Cell and Environment*, *18*(4), 339–355. https://doi.org/10.1111/j.1365-3040.1995.tb00370.x

Levis, S., Wiedinmyer, C., Bonan, G. B., & Guenther, A. (2003). Simulating biogenic volatile organic compound emissions in the Community Climate System Model. *Journal of Geophysical Research*, *108*(D21), 4659. https://doi.org/10.1029/2002JD003203

Li, C., Frolking, S., & Frolking, T. A. (1992). A model of nitrous oxide evolution from soil driven by rainfall events: 1. Model structure and sensitivity. *Journal of Geophysical Research*, *97*(9), 9759–9776. https://doi.org/10.1029/92JD00509

Li, L., Wang, Y., Zheng, Y., & Chen, T. (2018). Estimation of BVOC emissions in Guangzhou and its spatial-temporal variations: Preliminary results from GLOBEIS. In L. Wu, J. B. Cohen, D. Loyola, H. Letu, & K. Qin(Eds.), *ISPRS workshop on remote sensing and synergic analysis on atmospheric environment* (pp. 33–38). Copernicus Publications. https://doi.org/10.5194/isprs-archives-XLII-3-W5-33-2018

Malone, S. C., Weaver, D. K., Seipel, T. F., Menalled, F. D., Hofland, M. L., Runyon, J. B., et al. (2020). Herbivore-induced volatile emissions are altered by soil legacy effects in cereal cropping systems. *Plant and Soil*, *455*(1), 171–186. https://doi.org/10.1007/s11104-020-04674-2

Manco, A., Brilli, F., Famulari, D., Gasbarra, D., Gioli, B., Vitale, L., et al. (2021). Cross-correlations of Biogenic Volatile Organic Compounds (BVOC) emissions typify different phenological stages and stressful events in a Mediterranean Sorghum plantation. *Agricultural and Forest Meteorology*, *303*, 108380. https://doi.org/10.1016/j.agrformet.2021.108380

Massad, R.-S., Tuzet, A., & Bethenod, O. (2007). The effect of temperature on C4-type leaf photosynthesis parameters. *Plant, Cell and Environment*, *30*(9), 1191–1204. https://doi.org/10.1111/j.1365-3040.2007.01691.x

McEwan, M., & MacFarlane Smith, W. H. (1998). Identification of volatile organic compounds emitted in the field by oilseed rape (*Brassica napus* ssp. oleifera) over the growing season. *Clinical and Experimental Allergy*, *28*(3), 332–338. https://doi.org/10.1046/j.1365-2222.1998.00234.x

Monson, R. K., Jones, R. T., Rosenstiel, T. N., & Schnitzler, J.-P. (2013). Why only some plants emit isoprene. *Plant, Cell and Environment*, *36*(3), 503–516. https://doi.org/10.1111/pce.12015

Morfopoulos, C., Sperlich, D., Peñuelas, J., Cubells, I. F., Llusià, J., Medlyn, B. E., et al. (2014). A model of plant isoprene emission based on available reducing power captures responses to atmospheric CO_2. *New Phytologist*, *203*(1), 125–139. https://doi.org/10.1111/nph.12770

Morrison, E. C., Drewer, J., & Heal, M. R. (2016). A comparison of isoprene and monoterpene emission rates from the perennial bioenergy crops short-rotation coppice willow and *Miscanthus* and the annual arable crops wheat and oilseed rape. *Global Change Biology Bioenergy*, *8*(1), 211–225. https://doi.org/10.1111/gcbb.12257

Mozaffar, A., Schoon, N., Bachy, A., Digrado, A., Heinesch, B., Aubinet, M., et al. (2018). Biogenic volatile organic compound emissions from senescent maize leaves and a comparison with other leaf developmental stages. *Atmospheric Environment*, *176*, 71–81. https://doi.org/10.1016/j.atmosenv.2017.12.020

Müller, K., Pelzing, M., Gnauk, T., Kappe, A., Teichmann, U., Spindler, G., et al. (2002). Monoterpene emissions and carbonyl compound air concentrations during the blooming period of rape (*Brassica napus*). *Chemosphere*, *49*(10), 1247–1256. https://doi.org/10.1016/S0045-6535(02)00610-0

Nichol, J., & Wong, M. S. (2011). Estimation of ambient BVOC emissions using remote sensing techniques. *Atmospheric Environment*, *45*(17), 2937–2943. https://doi.org/10.1016/j.atmosenv.2011.01.028

Niinemets, Ü., & Monson, R. K. (2013). State-of-the-art of BVOC research: What do we have and what have we missed? A synthesis. In Ü. Niinemets, & R. K. Monson(Eds.), *Biology, controls and models of tree volatile organic compound emissions* (pp. 509–528). Springer. https://doi.org/10.1007/978-94-007-6606-8_18

Niinemets, Ü., Tenhunen, J. D., Harley, P. C., & Steinbrecher, R. (1999). A model of isoprene emission based on energetic requirements for isoprene synthesis and leaf photosynthetic properties for *Liquidambar* and *Quercus*. *Plant, Cell and Environment*, *22*(11), 1319–1335. https://doi.org/10.1046/j.1365-3040.1999.00505.x

Okumura, M., Kosugi, Y., & Tani, A. (2018). Biogenic volatile organic compound emissions from bamboo species in Japan. *Journal of Agricultural Meteorology*, *74*(1), 40–44. https://doi.org/10.2480/agrmet.D-17-00017

Pańka, D., Piesik, D., Jeske, M., & Baturo-Cieśniewska, A. (2013). Production of phenolics and the emission of volatile organic compounds by perennial ryegrass (*Lolium perenne* L.)/*Neotyphodium lolii* association as a response to infection by *Fusarium poae*. *Journal of Plant Physiology*, *170*(11), 1010–1019. https://doi.org/10.1016/j.jplph.2013.02.009

Peeters, J., Boullart, W., Pultau, V., Vandenberk, S., & Vereecken, L. (2007). Structure−Activity relationship for the addition of OH to (Poly)alkenes: Site-specific and total rate constants. *The Journal of Physical Chemistry A*, *111*(9), 1618–1631. https://doi.org/10.1021/jp066973o

Peñuelas, J., Asensio, D., Tholl, D., Wenke, K., Rosenkranz, M., Piechulla, B., et al. (2014). Biogenic volatile emissions from the soil. *Plant, Cell and Environment*, *37*(8), 1866–1891. https://doi.org/10.1111/pce.12340

Peñuelas, J., & Staudt, M. (2010). BVOCs and global change. *Trends in Plant Science*, *115*(3), 133–144. https://doi.org/10.1016/j.tplants.2009.12.005

Petersen, K., Kraus, D., Calanca, P., Semenov, M. A., Butterbach-Bahl, K., & Kiese, R. (2021). Dynamic simulation of management events for assessing impacts of climate change on pre-alpine grassland productivity. *European Journal of Agronomy*, *128*, 126306. https://doi.org/10.1016/j.eja.2021.126306

Piccot, S. D., Watson, J. J., & Jones, J. W. (1992). A global inventory of volatile organic compound emissions from anthropogenic sources. *Journal of Geophysical Research*, *97*(D9), 9897–9912. https://doi.org/10.1029/92JD00682

Pierce, T., Geron, C., Bender, L., Dennis, R., Tonnesen, G., & Guenther, A. (1998). Influence of increased isoprene emissions on regional ozone modeling. *Journal of Geophysical Research*, *103*(D19), 25611–25629. https://doi.org/10.1029/98JD01804

Porter, W. C., Barsanti, K. C., Baughman, E. C., & Rosenstiel, T. N. (2012). Considering the air quality impacts of bioenergy crop production: A case study involving *Arundo donax*. *Environmental Science & Technology*, *46*(17), 9777–9784. https://doi.org/10.1021/es3013084

Poupkou, A., Melas, D., Ziomas, I., Symeonidis, P., Lisaridis, I., Gerasopoulos, E., et al. (2009). Simulated summertime regional gound-level ozone concentrations over Greece. *Water, Air, & Soil Pollution*, *196*(1–4), 169–181. https://doi.org/10.1007/s11270-008-9766-0

Sarkar, C., Guenther, A. B., Park, J. H., Seco, R., Alves, E., Batalha, S., et al. (2020). PTR-TOF-MS eddy covariance measurements of isoprene and monoterpene fluxes from an eastern Amazonian rainforest. *Atmospheric Chemistry and Physics*, *20*(12), 7179–7191. https://doi.org/10.5194/acp-20-7179-2020

Saunders, S. M., Jenkin, M. E., Derwent, R. G., & Pilling, M. J. (2003). Protocol for the development of the master chemical mechanism, MCM v3 (Part A): Tropospheric degradation of non-aromatic volatile organic compounds. *Atmospheric Chemistry and Physics*, *3*, 161–180. https://doi.org/10.5194/acp-3-161-2003

Scott, C. E., Rap, A., Spracklen, D. V., Forster, P. M., Carslaw, K. S., Mann, G. W., et al. (2014). The direct and indirect radiative effects of biogenic secondary organic aerosol. *Atmospheric Chemistry and Physics*, *14*, 447–470. https://doi.org/10.5194/acp-14-447-2014

Simon, H., Fallmann, J., Kropp, T., Tost, H., & Bruse, M. (2019). Urban trees and their impact on local ozone concentration—a microclimate modeling study. *Atmosphere*, *10*(3), 154. https://doi.org/10.3390/atmos10030154

Simon, V., Dumergues, L., Ponche, J. L., & Torres, L. (2006). The biogenic volatile organic compounds emission inventory in France: Application to plant ecosystems in the Berre-Marseilles area (France). *The Science of the Total Environment*, *372*(1), 164–182. https://doi.org/10.1016/j.scitotenv.2006.08.019

Simpson, D., Winiwarter, W., Börjesson, G., Cinderby, S., Ferreiro, A., Guenther, A., et al. (1999). Inventorying emissions from nature in Europe. *Journal of Geophysical Research*, *104*(D7), 8113–8152. https://doi.org/10.1029/98JD02747

Sindelarova, K., Granier, C., Bouarar, I., Guenther, A., Tilmes, S., Stavrakou, T., et al. (2014). Global dataset of biogenic VOC emissions calculated by the MEGAN model over the last 30 years. *Atmospheric Chemistry and Physics*, *14*(7), 9317–9341. https://doi.org/10.5194/acp-14-9317-2014

Sommer, M., Augustin, J., & Kleber, M. (2016). Feedbacks of soil erosion on SOC patterns and carbon dynamics in agricultural landscapes - the CarboZALF experiment. *Soil and Tillage Research*, *156*, 182–184. https://doi.org/10.1016/j.still.2015.09.015

Song, C., Liu, B., Dai, Q., Li, H., & Mao, H. (2019). Temperature dependence and source apportionment of volatile organic compounds (VOCs) at an urban site on the north China plain. *Atmospheric Environment*, *207*, 167–181. https://doi.org/10.1016/j.atmosenv.2019.03.030

Spielmann, F. M., Langebner, S., Ghirardo, A., Hansel, A., Schnitzler, J.-P., & Wohlfahrt, G. (2017). Isoprene and α-pinene deposition to grassland mesocosms. *Plant and Soil*, *410*(1), 313–322. https://doi.org/10.1007/s11104-016-3009-8

Street, R. A., Duckham, S. C., Boissard, C., Hewitt, C. N., & Slanina, S. (1997). Emissions of VOCs from stressed and unstressed vegetation. In *Biosphere-atmosphere exchange of pollutants and trace substances* (pp. 366–371). Springer.

Szogs, S., Arneth, A., Anthoni, P., Doelman, J. C., Humpenöder, F., Popp, A., et al. (2017). *Impact of LULCC on the Emission of BVOCs during the 21st Century*. Atmospheric Environment. (Vol. 165, pp. 73–87). https://doi.org/10.1016/j.atmosenv.2017.06.025

Thornley, J. H. M. (2002). Instantaneous canopy photosynthesis: Analytical expressions for sun and shade leaves based on exponential light decay down the canopy and an acclimated non-rectangular hyperbola for leaf photosynthesis. *Annals of Botany*, *89*(4), 451–458. https://doi.org/10.1093/aob/mcf071

Thornley, J. H. M., & Cannell, M. G. R. (2000). Modelling the components of plant respiration: Representation and realism. *Annals of Botany*, *85*, 55–67. https://doi.org/10.1006/anbo.1999.0997

Usseglio, V. L., Pizzolitto, R. P., Rodriguez, C., Zunino, M. P., Zygadlo, J. A., Areco, V. A., et al. (2017). Volatile organic compounds from the interaction between *Fusarium verticillioides* and maize kernels as a natural repellents of *Sitophilus zeamais*. *Journal of Stored Products Research*, *73*(Supplement C), 109–114. https://doi.org/10.1016/j.jspr.2017.08.001

Von Caemmerer, S. (2000). *Biochemical models of leaf photosynthesis*. CSIRO. (p. 165). https://doi.org/10.1071/9780643103405

Wang, C. T., Wiedinmyer, C., Ashworth, K., Harley, P. C., Ortega, J., Rasool, Q. Z., et al. (2019). Potential regional air quality impacts of cannabis cultivation facilities in denver, Colorado. *Atmospheric Chemistry and Physics*, *19*(2), 13973–13987. https://doi.org/10.5194/acp-19-13973-2019

Wang, N., Kostenidou, E., Donahue, N. M., & Pandis, S. N. (2018). Multi-generation chemical aging of α-pinene ozonolysis products by reactions with OH. *Atmospheric Chemistry and Physics*, *18*(5), 3589–3601. https://doi.org/10.5194/acp-18-3589-2018

Wiß, F., Ghirardo, A., Schnitzler, J.-P., Nendel, C., Augustin, J., Hoffmann, M., & Grote, R. (2017). Net ecosystem fluxes and composition of BVOCs over a maize field - interaction of meteorology and phenological stages. *GCB Bioenergy*, *9*(11), 1627–1643. https://doi.org/10.1111/gcbb.12454

Wu, K., Yang, X., Chen, D., Gu, S., Lu, Y., Jiang, Q., et al. (2020). Estimation of biogenic VOC emissions and their corresponding impact on ozone and secondary organic aerosol formation in China. *Atmospheric Research*, *231*, 104656. https://doi.org/10.1016/j.atmosres.2019.104656

Yin, X., Van Oijen, M., & Schapendonk, H. C. M. (2004). Extension of a biochemical model for the generalized stoichiometry of electron transport limited C_3 photosynthesis. *Plant, Cell and Environment*, *27*, 1211–1222. https://doi.org/10.1111/j.1365-3040.2004.01224.x

Yu, G.-R., Zhuang, J., & Yu, Z.-L. (2001). An attempt to establish a synthetic model of photosynthesis-transpiration based on stomatal behavior for maize and soybean plants grown in field. *Journal of Plant Physiology*, *158*(7), 861–874. https://doi.org/10.1078/0176-1617-00177

Zhao, K., Bao, Y., Huang, J., Wu, Y., Moshary, F., Arend, M., et al. (2019). A high-resolution modeling study of a heat wave-driven ozone exceedance event in New York City and surrounding regions. *Atmospheric Environment*, *199*, 368–379. https://doi.org/10.1016/j.atmosenv.2018.10.059

Zheng, J., Zheng, Z., Yu, Y., & Zhong, L. (2010). Temporal, spatial characteristics and uncertainty of biogenic VOC emissions in the Pearl River Delta region, China. *Atmospheric Environment*, *44*(16), 1960–1969. https://doi.org/10.1016/j.atmosenv.2010.03.001